Molecular Diversity
https://doi.org/10.1007/s11030-018-9867-7

ORIGINAL ARTICLE

Design, synthesis, and in silico studies of novel eugenyloxy propanol azole derivatives having potent antinociceptive activity and evaluation of their β-adrenoceptor blocking property

Somayeh Behrouz[1] · Mohammad Navid Soltani Rad[1] · Bahareh Taghavi Shahraki[1] · Mohammad Fathalipour[2] · Marzieh Behrouz[1] · Hossein Mirkhani[2]

Received: 16 April 2018 / Accepted: 2 August 2018

Abstract
The design, synthesis, antinociceptive and β-adrenoceptor blocking activities of several eugenyloxy propanol azole derivatives have been described. In this synthesis, the reaction of eugenol with epichlorohydrin provided adducts **3** and **4** which were *N*-alkylated by diverse azoles to obtain the eugenyloxy propanol azole analogues in good yields. Adducts **3** and **4** were also reacted with azide ion to obtain the corresponding azide **6**. The 'Click' Huisgen cycloaddition reaction of **6** with diverse alkynes afforded the title compounds in good yields. The synthesized eugenyloxy propanol azole derivatives were in vivo studied for the acute antinociception on male Spargue Dawley rats using tail-flick test. Compounds **5f**, **5g**, **7b** and **11a** exhibited potent analgesic properties in comparison with eugenol as a standard drug. In addition, all compounds were ex vivo tested for β-adrenoceptor blocking properties on isolated left atrium of male rats which exhibited partial antagonist or agonist behaviour compared to the standard drugs. The molecular docking study on the binding site of transient receptor potential vanilloid subtype 1 (TRPV1) has indicated that like capsaicin, eugenyloxy propanol azole analogues exhibited the strong affinity to bind at site of TPRV1 in a "tail-up, head-down" conformation and the presence of triazolyl moieties has played undeniable role in durable binding of these ligands to TRPV1. The in silico pharmacokinetic profile, drug likeness and toxicity predictions carried out for all compounds determined that **5g** can be considered as potential antinociceptive drug candidate for future research.

Keywords Eugenol · Eugenyloxy propanol azole · Antinociceptive · β-Adrenoceptor · Antagonist · Agonist

Introduction

Through the history of human life, pain is known as a global severe problem. As an instance in USA, 3 million adults suffer from daily pain [1]. Pain is an unpleasant sensory and emotional experience associated with actual or potential tissue damage [2]. Although the pain is diseases' symptom, pain extensively diminishes the quality of life and also costs a lot to human society. Up to now, diverse classes of analgesic drugs are in use; nevertheless, they exhibit a wide range of side effects. Thus, the search for the new therapeutic alternatives is critically essential.

Natural products provide a diverse and unique source of lead compounds for drug discovery [3]. Naturally occurring eugenol (4-allyl-2-metoxy-phenol) is known biological active phenolic ingredient found in essential oils of diverse plants majorly in clove oil (*Eugenia caryophyllata*) [4]. Eugenol has been extensively applied in medicine especially in dentistry due to its analgesic and antiseptic properties upon mixing with zinc oxide (ZOE) which is utilized as cement for temporary fillings of the teeth [5]. In addition to its traditional applications as both analgesic and antiseptic drug, eugenol is

Electronic supplementary material The online version of this article (https://doi.org/10.1007/s11030-018-9867-7) contains supplementary material, which is available to authorized users.

✉ Somayeh Behrouz
behrouz@sutech.ac.ir

✉ Mohammad Navid Soltani Rad
soltani@sutech.ac.ir

[1] Medicinal Chemistry Research Laboratory, Department of Chemistry, Shiraz University of Technology, Shiraz 71555-313, Iran

[2] Faculty of Pharmacy, Shiraz University of Medical Science, Medicinal and Natural Products Chemistry Research Center, P.O.Box 71345-1149, Shiraz, Iran

Published online: 09 August 2018

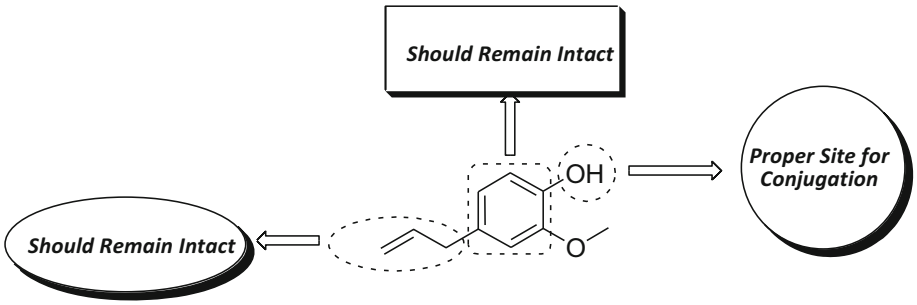

Fig. 1 Structure of eugenol and proper site for conjugation

known for its different biological activities. They comprise anti-inflammatory [6], antispasmodic [6], hepatoprotective [6], antianaphylactic [7], antiplatelet [7], antipyretic [7], antifungal [8], antiviral [9], antidepressant [10], anti-oxidant [10], antibacterial [11], acaricidal [12], antihelicobacter [13] and antiproliferative properties [14]. Given the significance and prominent pharmaceutical properties of eugenol, it was extensively used to design and synthesize the potentially biologically active compounds. One way to acquire the new eugenol derivatives is the conjugation with various functionalities, molecules and/or other drugs [15–17]. However, the biological assessments on these eugenol derivatives have revealed that the therapeutic activity is mostly observed when the eugenol is conjugated with diverse functionalities through its free hydroxyl moiety (Fig. 1) [16, 17]. In this connection, a few hybrid molecules **I–XIII** having a eugenyloxy core were reported by different research teams [18–31]. The chemical structures and biological activities of compounds I–XIII are depicted in Fig. 2.

Hypertension is called the silent killer since most patients with high blood pressure have no symptoms to alert them [32]. Untreated hypertension increases the risk of heart disease and stroke. Hypertension can also damage the kidneys and increase the risk of blindness and dementia [33]. Regarding to the importance of this dangerous disease, the extensive efforts were made to find the potent and novel therapeutic agents for hypertension remedy in recent years [34]. To overcome the hypertension, antagonizing the β-adrenoceptors with β-blockers is a decisive and effective way [35]. Among β-blockers known for the inhibition of β-adrenergic receptors, aryloxypropanolamine is most known and distinguished compounds (Fig. 3) [36]. The structural activity relationship (SAR) assessments of aryloxypropanolamines have revealed that they are very homogeneous in pattern as the majority of them exhibit the incumbent pharmacophores comprising aryloxy, amine and hydroxypropyl moieties [37]. Up to now, a great deal of aryloxypropanolamines have been synthesized where many of them are now approved drugs and largely prescribed for hypertension remedy [38]. To improve the aryloxypropanolamines activity, the strategy in ring variations was applied and in this connection various aryloxy moieties were considered. As instance, incorporation of naturally occurring guaiacol and 2-allyl phenol was led to discovery of moprolol and alprenolol, respectively. Chen and coworkers [22, 31] demonstrated that the combination of methoxy and allyl residues in phenolic part as a eugenolyl moiety was led to potent β-blockers (**V**) and (**XIII**) (Fig. 2).

In most of known β-blockers involving aryloxypropanolamine framework, the variation is generally conducted in aromatic cores, whereas the alteration in amine residues is mostly restricted to simple branched aliphatic amines [38]. In this context, it was proved that the extension of amino group and/or incorporation of long and bulky amine substituents in aryloxypropanolamine structure can extensively improve the selectivity towards β-adrenoceptores [39]. In line with our interest in design and synthesis of new aryloxypropanolamines [40–44], herein we would like to report the synthesis, antinociceptive and β-blocking studies of eugenyloxy propanol azole derivatives (Fig. 4) as new analogues of compounds (**V**) and (**XIII**) in which the azole cores are surrogated instead of amine residues in (**V**) and (**XIII**).

Results and discussion

Chemistry

The synthesis of title compounds followed the general pathway demonstrated in Scheme 1. As shown in Scheme 1, the first step includes the reaction of eugenol (**1**) with epichlorohydrin (**2**) which was achieved in the presence of K_2CO_3 as a base and a catalytic amount of tetrabutylammonium iodide (TBAI) in anhydrous acetonitrile at reflux condition. After the reaction completion, a mixture of chlorohydrin (**3**) and epoxide (**4**) was afforded as major and minor products, respectively.

Without requiring to separate **3** from **4**, the crude mixture was subsequently prepared to react with diverse *N*-heterocyclic compounds comprising azole and imide derivatives using a basic mixture of K_2CO_3 and triethylamine (TEA) and a catalytic amount of TBAI in anhydrous acetonitrile at reflux condition (Scheme 1a). The structures of *N*-heterocyclic compounds used to prepare **5a–g** are depicted

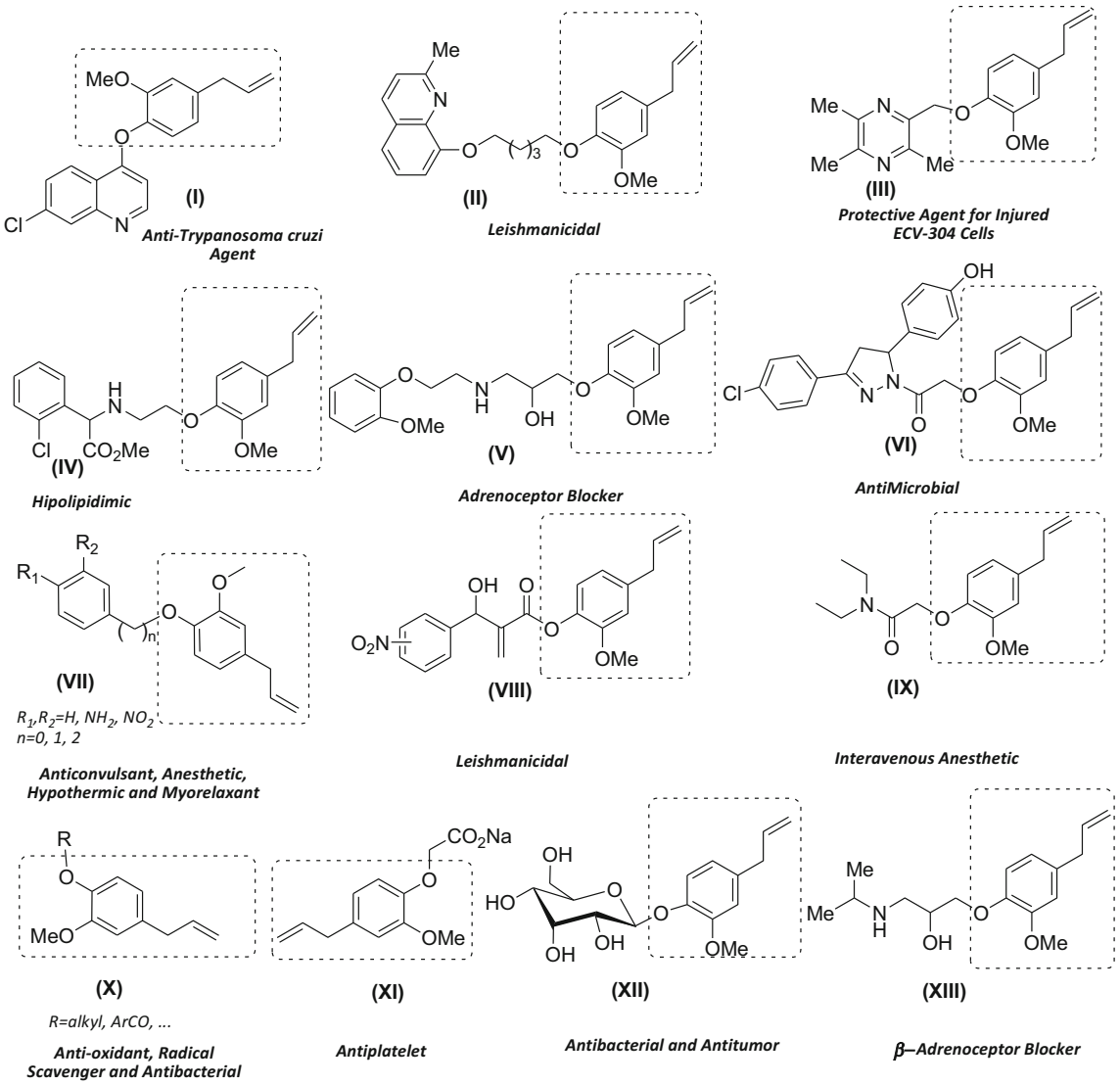

Fig. 2 Structure and biological behaviours of some hybrid molecules having eugenyloxy core

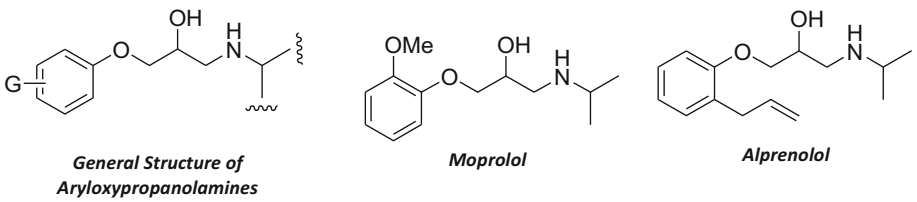

Fig. 3 General structure of aryloxypropanolamine, moporol, and alprenolol

in Scheme 1a. To involve the 1,2,3-triazolyl cores as the surrogates for *N*-heterocyclic residues inside **5a–g** structures, a mixture of (**3**) and (**4**) underwent the azidation reaction using sodium azide in acetone–water solution at reflux condition which led to 1-(4-allyl-2-methoxy-phenoxy)-3-azido-propan-2-ol (**6**) (Scheme 1b). β-Azido alcohol **6** is a proper starting material for Huisgen's azide-alkyne cycloaddition. In this connection, azide **6** was used to react with diverse alkynes through Cu(I)-catalysed azide-alkyne cycloaddition (CuAAC) in the presence of catalytic amount of CuI in H_2O-THF (1:1) media at ambient temperature. Two different types of terminal alkynes were employed to access the corresponding 1,2,3-triazolyl derivatives including, (1) commercially available terminal alkynes having simple substituents (Scheme 1b) and (2) commercially unavailable terminal alkynes bearing diverse *N*-heterocyclic compounds (Scheme 1c). The later alkynes were synthesized from the propargyl tosylate (**9**) that was easily obtained from tosy-

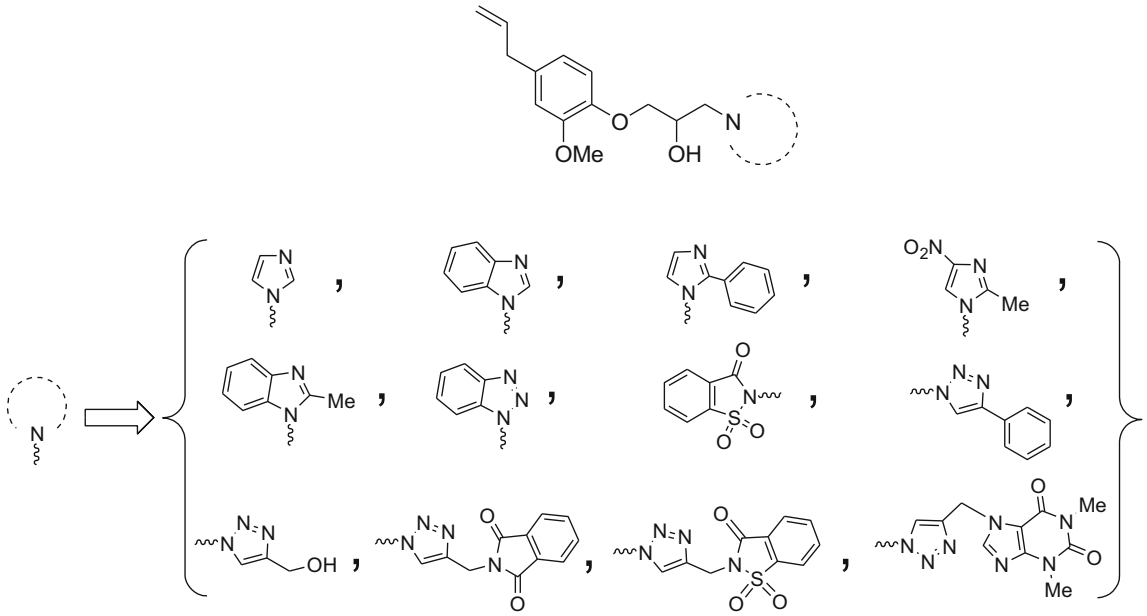

Fig. 4 General structure of new eugenyloxy propanol azole derivatives

lation of propargyl alcohol (**8**) due to modified reported procedure [45] (Scheme 1c). The obtained **9** was then used to react with diverse *N*-heterocyclic compounds to yield alkyne (**10**). All alkynes were readily converted to their corresponding 1,2,3-triazolyl derivatives (**7a,b**,**11a–c**) utilizing CuAAC reaction in good yields (Table 1).

Antinociceptive activity

Acute antinociception was studied by tail-flick test. The analgesic response of compounds was carried out using the tail-flick apparatus (Sanat Azma, Iran). Rats were restrained in a plexiglass cylinder, and radiant heat was focused from a distance of 4–7 cm on the distal end of the tail [46]. Time of latency was determined three times for each rat, and their mean was considered as baseline latency before compounds treatment. The intensity of the light was adjusted to produce mean baseline latency time between 3 and 5 s. The cut-off time was fixed at 10 s to avoid tissue damage. After baseline latencies were established, rats were treated with an intraperitoneal injection of vehicle (15% DMSO/saline), eugenol and synthesized compounds (100 mg/kg), and the latency time was measured at 15, 30, 45 and 60 min after injection [47, 48]. The latencies were converted to the percentage of antinociception (% Maximal Possible Effect) according to the following equation [49, 50]:

$$\%\text{Antinociception (\%MPE)} = \left[(\text{Latency time of compound} - \text{baseline latency time}) / (\text{cut-off time-basal response time})\right] \times 100$$

Time-dependent antinociceptive response (MPE vs time) of eugenyloxy propanol azole derivatives, vehicle and pure eugenol as a standard analgesic drug on the tail-flick assay is shown in Fig. 5. As can be seen in Fig. 5a, none of compounds **5a–c** have displayed analgesic property in comparison with eugenol at examined times; however, among **5d–f** (Fig. 5b), compound **5f** demonstrates the best analgesic profile at all exposure times compare to eugenol. The maximal analgesic potency for **5f** with MPE around 64% at 15 min was observed, whereas eugenol exhibited MPE value around 26% at the same exposure time. Compound **5e** showed nearly an equal analgesic strength at 15 min test time compared to eugenol, instead of its weaker activity profile at other tested times. Additionally, both compounds **5g** and **7b** were determined to have higher MPE values at all studied times and thus exhibited stronger analgesic performance than eugenol (Fig. 5c). Antinociception mediated by **7a** was merely observed at 15-min exposure time with a higher MPE value (33%) compare to eugenol (Fig. 5c). Among compounds **11a–c**, **11a** displayed considerable antinociception activity at all investigated times (Fig. 5d). The highest analgesic activity for **11a** was observed at 30 min with a MPE value around 58%. Similarly to **7a**, also **11b** revealed a higher antinociception at 15 min as compared to eugenol. Finally, **11c** involved nearly an equal antinociception behaviour at 45 min (Fig. 5d). Since the general presence of eugenyloxy propanolyl moiety in all synthesized compounds, the difference in antinociception activities is attributed to the alteration in tethered *N*-heterocyclic cores. Regarding obtained data and also the variation in structure of title compounds, it is well revealed that the presence of 1,2,3-triazolyl moieties

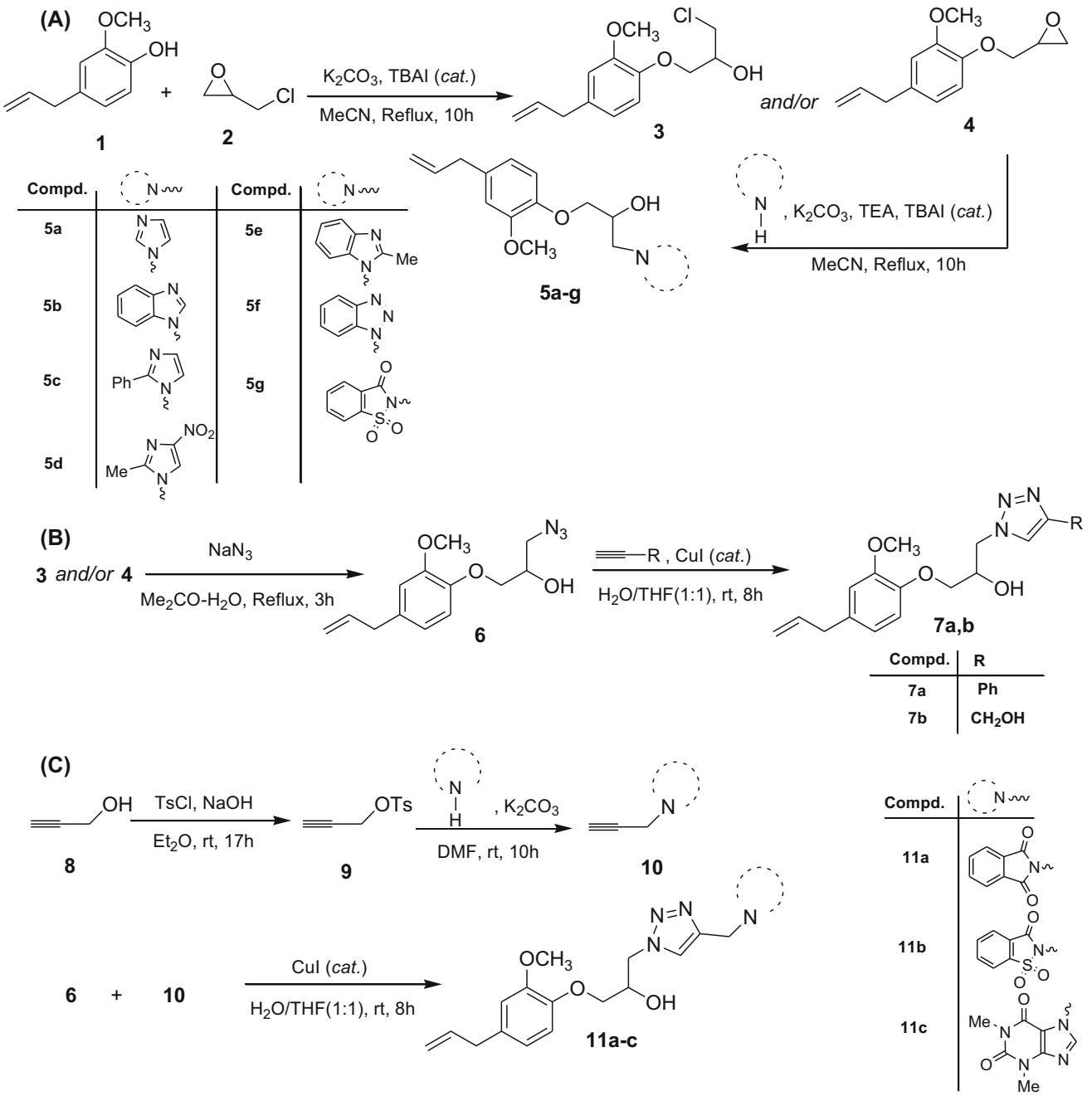

Scheme 1 Synthesis of eugenyloxy propanol azole derivatives: **a** via direct *N*-alkylation of azoles; **b** Huisgen's azide-alkyne cycloaddition using commercially available alkynes; and/or **c** Huisgen's azide-alkyne cycloaddition using commercially unavailable alkynes

extensively enhances the antinociceptive potency of synthesized compounds.

β-Adrenoceptor studies

Tissue studies

The effect of title compounds was examined on isolated left atrium of male rats. Left atria were dissected free from the hearts of anaesthetized rats and mounted between two stainless steel electrodes in organ bath witch filled by 20 mL of physiological salt solution (PSS) with the following composition (mM): NaCl (119), KCl (4), KH_2PO_4 (1.2), $CaCl_2$ (3.3), $MgSO_4$ (2.4), $NaHCO_3$ (25), and D-glucose (11). The solution was bubbled continuously with a carbogen mixture (5% CO_2) at temperature 37 °C and pH 7.4 [51].

The atria were paced by the stimulation (frequency 1 Hz, pulse width 5 ms and voltage 20% above threshold). The resting tension was adjusted to 0.5 g for a stability period of 30 min which the solution was exchanged every 10 min.

Table 1 List of synthesized novel eugenyloxy propanol azole derivatives

Compound[a]	mp (°C)	Yield (%)[b]
5a	Oil	75
5b	127–129	82
5c	Oil	76
5d	106–108	78
5e	155–157	80
5f	40–42	69
5g	Foam	80
7a	96–98	78
7b	80–82	75
11a	97–99	80
11b	Foam	83
11c	100–102	84

[a]All products were characterized by ^{1}H and ^{13}C NMR, IR, CHN, and MS analysis
[b]Isolated yield

The tension was recorded with an isometric force transducer (K 30, Hugo Sachs Elektronik, Germany) on a PC software (HSE-ACAD, Hugo Sachs Elektronik, Germany).

Study of β-antagonist and β-agonist activities

To examine the β-antagonist activity of title compounds on the atrial β-adrenergic receptors, initially, the isolated atria were exposed to the concentration of isoprenaline that increased initial stimulator-provoked contraction by 50% (EC_{150}). After washing out and maintaining the baseline contractions, the atria were pre-incubated with different concentrations of synthesized compounds or propranolol (1×10^{-10}–1×10^{-4} M) for 10 min. Thereafter, the tissues were exposed once again with EC_{150} of isoprenaline. Finally, the concentration–response curves of synthetic compounds and propranolol were plotted. The initial contraction percentage versus compounds' concentrations is shown in Fig. 6. As can be seen in Fig. 6, none of the synthesized compounds showed the remarkable antagonistic properties compared to propranolol as a reference β-antagonist. Unlike compounds **5a–g**, **11a** and **11b** exhibited antagonistic behaviour to some extent at different concentrations; however, other compounds involving **7a**, **7b** and **11c** essentially exhibited agonistic behaviour (Fig. 6).

In another set of experiments, the β-agonist activity of title compounds on the atrial β-adrenergic receptors was examined. To this end, the isolated left atria were exposed to concentrations of isoprenaline or synthetic compounds (1×10^{-10}–1×10^{-4} M) and increasing atrial contractions were

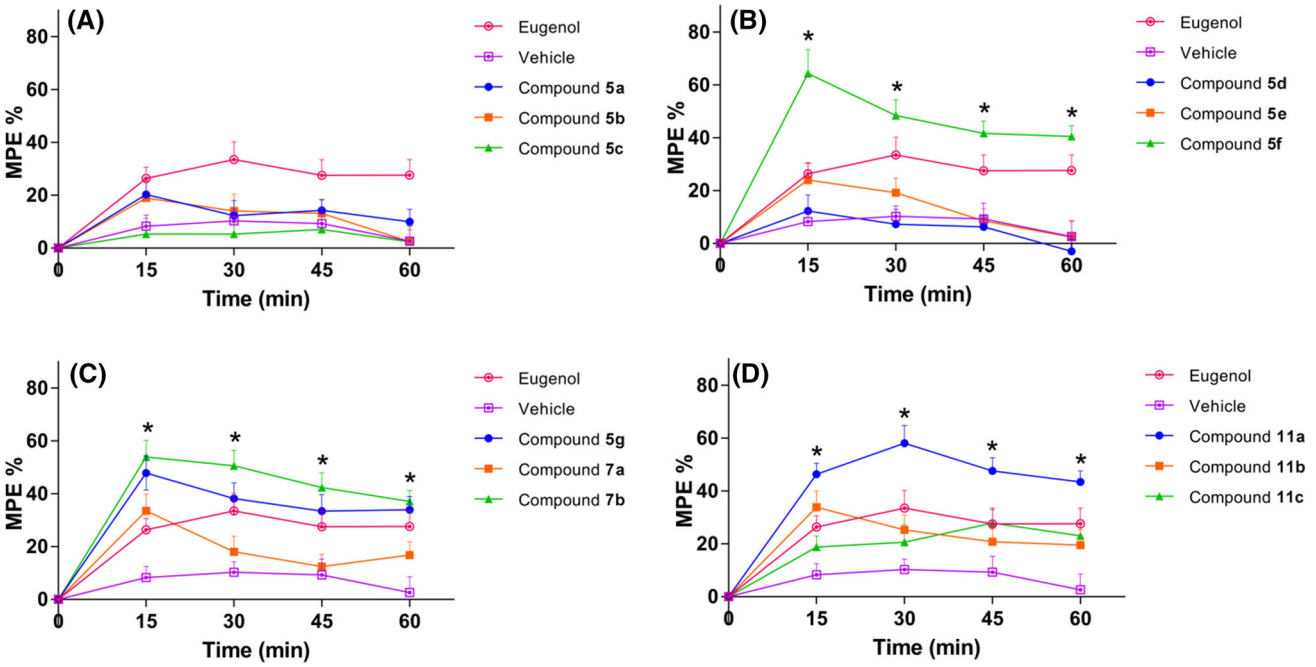

Fig. 5 Time-dependent antinociceptive response of vehicle, eugenol, and synthetized compounds on the tail-flick assay in rats. Compounds were administered intraperitoneally (100 mg/kg) into rats. All results were presented as mean ± SEM (n = 3–5/compound) of MPE (%). Comparisons were made by one-way ANOVA with Tukey post hoc test. Higher and statistical significance versus eugenol derivatives was depicted as $^{*}p < 0.05$

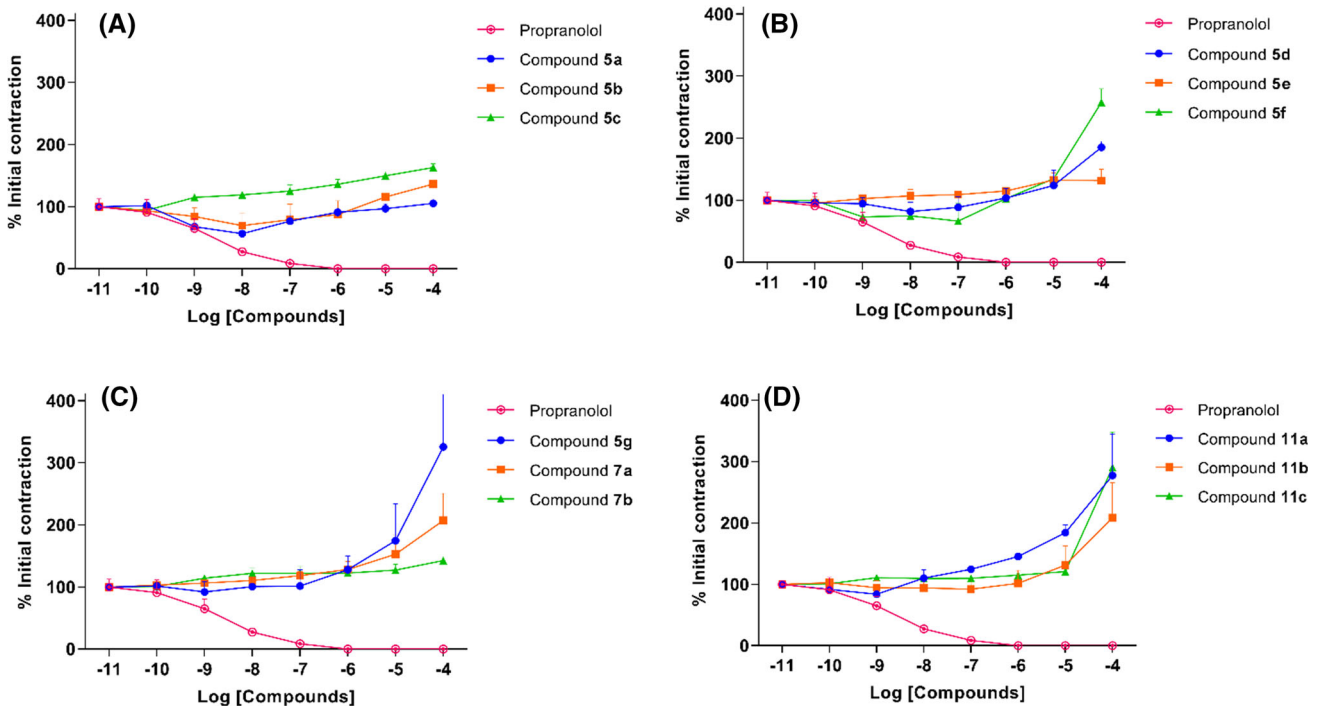

Fig. 6 Effect of different concentrations of synthesized compounds on the response of isolated rat atrium to EC_{50}-induced contraction of isoprenaline (100% contraction); each point represents the mean ± SEM ($n = 3$–5/compound)

recorded. Thereafter, the concentration–response curves of isoprenaline and synthetic compounds were plotted and their pEC_{50} (negative logarithm of the concentration that increased baseline contraction by 50%) and C_{max} (maximum contraction that produced at 1×10^{-4} M) were calculated. The initial contraction percentage versus compounds' concentrations is shown in Fig. 7. As specified in Fig. 7, all compounds exhibited lower initial contraction in comparison with isoprenaline as a reference agonist, and thus, they demonstrated the antagonistic properties. Table 2 indicates the potency and the maximum efficacy of synthesized compounds respect to isoprenaline on the response of isolated rat atrium. As indicated in this Table, among tested compounds, **5a** displayed less agonistic property than other examined compounds, whereas **5g** showed more maximum contraction (E_{max}) or agonistic property at a certain concentration (Table 2). In general, on the basis of both β-agonist and antagonist assessments (Figs. 6, 7), eugenyloxy propanol azole derivatives could be considered as partial antagonists or agonists.

Toxicity studies

Animals were cared for 5 days after administration of each compounds and no mortality rate was observed.

In silico studies

Molecular docking study

Transient receptor potential vanilloid subtype 1 (TRPV1) is a key transducer molecule of nociceptors which acts as a polymodal molecular pain receptor [52–54]. TRPV1 is a cation channel which has a vital effect in the molecular mechanisms responsible for pain hypersensitivity and injury-related hyperalgesia [55]. The activation of TRPV1 channel can be considered as an attractive strategy for pain therapy. Generally, this is achieved by various stimuli including acidic *p*H, heat, several inflammatory mediators and a wide range of vanilloids [52–54]. Particularly, the activation of TRPV1 by capsaicin, the spicy component of chili pepper, is well established and studied. It was proved that TRPV1 which is present in nociceptive neurons act as a specific and selective receptor for capsaicin [56]. Accordingly, TRPV1 is also well known as the capsaicin receptor [57].

Recently, three-dimensional (3D) structure of TRPV1 has been determined using single-particle electron cryo-microscopy (cryo-EM) experiments [58]. TRPV1 channels are homotetramers around a central permeation pore and have transmembrane topology resembling that of voltage-gated ion channels [58]. Each subunit consists of six transmembrane helices (S1–S6) plus a re-entrant loop-helix domain between S5 and S6. Based on the mutagenesis studies, four

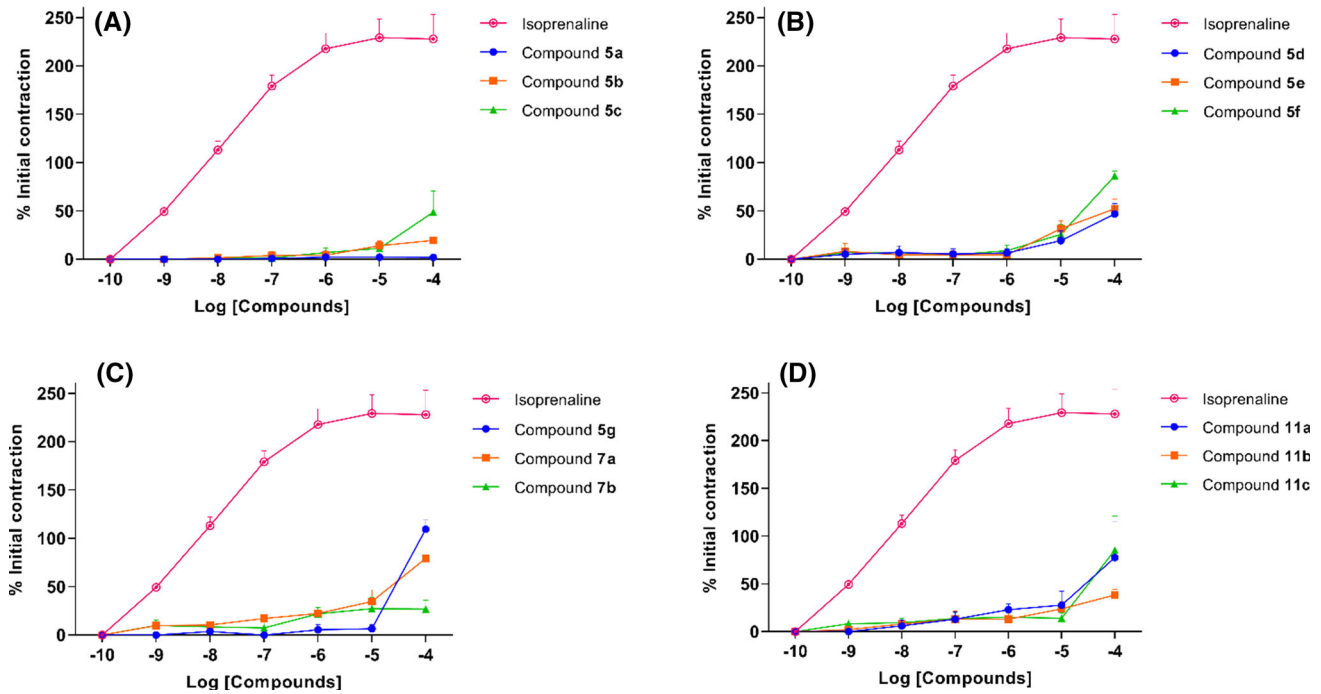

Fig. 7 Effect of different concentrations of isoprenaline and synthesized compounds on the response of isolated rat atrium; each point represents the mean ± SEM (n = 3–5/compound)

Table 2 Potency and maximum efficacy of isoprenaline and synthetic compounds on the response of isolated rat atrium

Compounds	pEC_{50}[b]	E_{max} (%)[d]	Compounds	pEC_{50}	E_{max} (%)
ISP[a]	9.0 ± 1.2	224.9 ± 25.4			
5a	NC[c]	2.1 ± 2.1	**5g**	4.7 ± 0.3	109.5 ± 9.5
5b	NC	19.6 ± 2.6	**7a**	5.0 ± 0.4	79.4 ± 1.6
5c	NC	48.9 ± 22.0	**7b**	NC	27.0 ± 9.2
5d	NC	46.8 ± 10.7	**11a**	4.5 ± 0.3	77.7 ± 38.1
5e	4.6 ± 0.2	52.4 ± 9.9	**11b**	NC	38.5 ± 6.1
5f	4.6 ± 0.1	86.3 ± 3.3	**11c**	4.4 ± 0.2	85.6 ± 35.9

Data are presented as the mean ± SEM (n = 3–5/compound)
[a]Isoprenaline
[b]pEC_{50}: negative logarithm of the concentration that increased baseline contraction by 50%
[c]Not calculated
[d]E_{max}: maximum contraction that produced at 1×10^{-4} M

residues play a significant role for specification of sensitivity to small vanilloid compounds. These residues include Tyr511 and Ser512 in S3 and Met547 and Thr550 in S4 [58]. The binding site of capsaicin is located at the interface between two monomers involving residues from S3 and S4 helices [58]. Recently, a "tail-up, head-down" conformation in the binding pocket was reported for the binding mode of capsaicin to the receptor which is known as the VR_{down} conformation [59]. Thus, the vanillyl ring (VR) of capsaicin points downward and towards the S4–S5 linker that provides an interaction with Tyr511. In addition, the aliphatic tail of capsaicin is upward and towards Phe543 in S4 helix providing nonspecific hydrophobic contacts with the channel.

The molecular docking study is a widely used computational method to study the binding mode and interactions of the ligand with the binding site of receptor or enzyme. Since our compounds demonstrated good to excellent profile of analgesic activity, the binding modes of the most potent compounds in the binding site of TRPV1 were investigated using a molecular docking study.

To this end, the structure of TRPV1 from Rattus norvegicus (PDB code: 3J5R) was selected as a template. The structure of 3J5R was taken from the Protein Data Bank (http://www.rcsb.org). The molecular docking study was performed using Molegro Virtual Docker (MVD) software without any change in its default settings [60]. The bind-

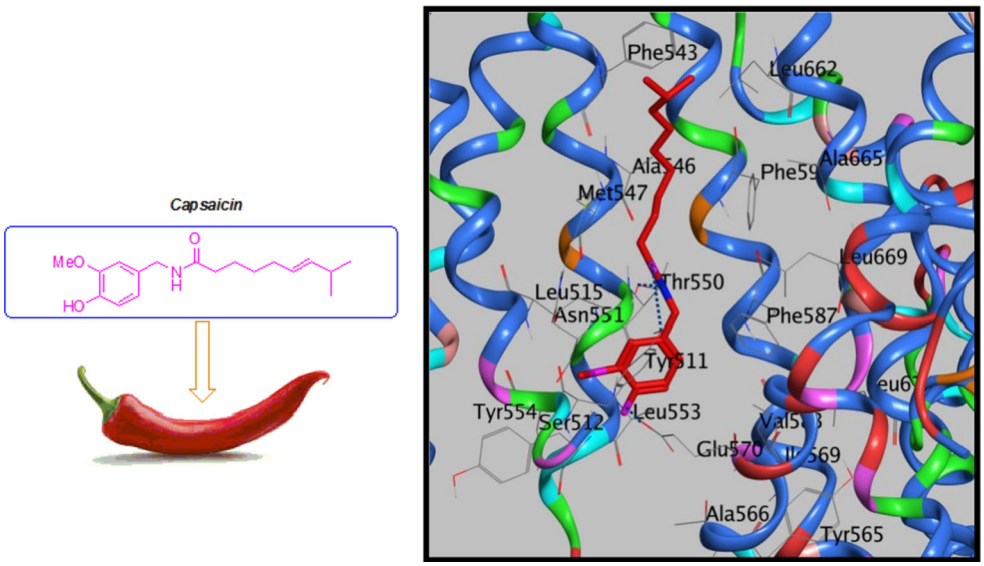

Fig. 8 Chemical structure, docked conformation and hydrogen bonds (dark blue) of capsaicin in binding site of TRPV1. (Color figure online)

ing site of the receptor was defined to comprise the residues within a 7 Å radius around the bound ligand. To obtain the optimized geometry of ligands **5f**, **5g**, **7b**, **11a**, and capsaicin, the DFT method at the B3LYP/6-31+G** level of theory using Gaussian 09 programme was employed [61].

In our initial attempt to perform the molecular docking study, the binding mode of capsaicin with TRPV1 (PDB code: 3J5R) was investigated, and the results were found to be similar to that reported in the literature [59]. The chemical structure of capsaicin and its binding geometry and interaction are depicted in Fig. 8.

It is clear from Fig. 8 that capsaicin has adopted the VR_{down} conformation since the vanillyl ring is pointing downward and in direction of Tyr511 and the hydrophobic tail is upward. In general, three types of interactions including electrostatic, hydrogen bond, and hydrophobic interactions play substantial role for binding the ligand to the receptor. Since capsaicin is neutral, the electrostatic interactions were not detected. However, both hydrogen bonding and hydrophobic interactions are important stabilizing features for suitable interaction of capsaicin with receptor. The aliphatic tail is involved in the hydrophobic interactions with the channel, and the polar groups such as amide moiety can easily achieve the hydrogen bonds with the appropriate amino acids. In this concern, three hydrogen bonds were perceived for interaction of capsaicin with TRPV1 including (1) the carbonyl moiety of amide from capsaicin with Tyr511 from S3, (2) the nitrogen atom of amide from capsaicin with Thr550 from S4, and (3) the OH residue of vanillyl ring with Glu570 in S4-S5 linker. In addition, two hydrophobic pockets contribute to the hydrophobic interaction with the vanillyl ring and the aliphatic tail of capsaicin. Thus, a hydrophobic cluster formed by Tyr511, Leu515, Leu553, Val583, Phe587, and Leu669 interacts with the vanillyl ring. The second hydrophobic pocket formed by Phe543, Ala546, Met547, Phe591, Leu662, and Ala665 anchors in the hydrophobic tail.

An overlay view of docked conformations of **5f**, **5g**, **7b**, **11a**, and capsaicin at the binding site of TRPV1 is shown in Fig. 9. Similarly with status of vanillyl ring in capsaicin at TPRV1 binding site, the eugenolyl rings of the above compounds stand at the same position. As expected, the docking results determined that the eugenolyl rings of ligands **5f**, **5g**, **7b**, and **11a** are oriented towards Tyr511 which is downward. Therefore, all of four docked ligands adopted the conformation similar to capsaicin which is known as the VR_{down} conformation.

The docked conformations and hydrogen bond interactions of **5f**, **5g**, **7b**, and **11a** are illustrated in Fig. 10. As shown in Fig. 10, all of docked ligands participate in several hydrogen bonds with TRPV1. In the case of **5f**, five strong hydrogen bonds were detected (Fig. 10a). The carbonyl group of Thr550 contributes to the hydrogen bond with hydroxyl residue of ligand. In addition, OH of Thr550 formed two hydrogen bonds with two nitrogens of triazole ring of **5f**. Also, these nitrogens participate in hydrogen bonds with OH of Tyr511. Both eugenolyl and benzotriazolyl groups of **5f** were involved in hydrophobic interactions with diverse amino acids including Tyr511, Leu515, Met547, Leu553, Ala566, Val583, Phe587, Phe591, Leu669.

The docked conformation of ligand **5g** is shown in Fig. 10b. As shown in Fig. 10b, ligand **5g** was located in the binding site of receptor and stabilized with three strong hydrogen bonds. The eugenolyl group participates in hydrogen bonds with hydroxyl moieties of Tyr511 and Thr550. The third hydrogen bond was formed between hydroxyl

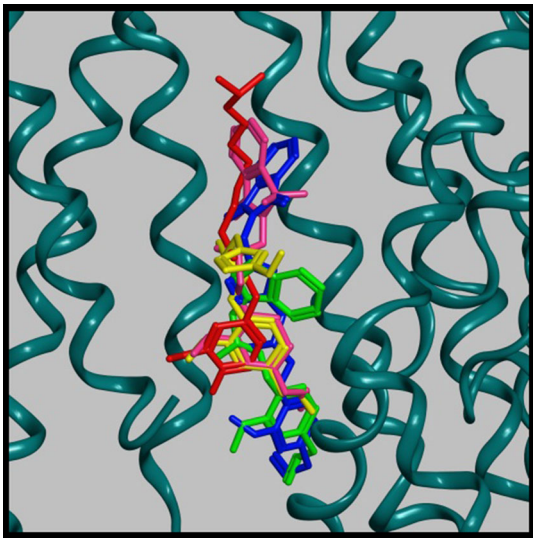

Fig. 9 Overlay view of docked conformations of **5f** (green), **5g** (pink), **7b** (yellow), **11a** (blue), and capsaicin (red) in binding site of TRPV1. (Color figure online)

residues of Thr550 and ligand. A hydrophobic cluster formed by Tyr511, Leu515, Leu553, Ala566, Val583, Phe587, and Leu669 anchors the eugenolyl group. In addition, the sacharinyl moiety interacts with the second hydrophobic pocket formed by Phe543, Ala546, Met547, Phe591, and Leu662.

The docking study of **7b** revealed that this ligand participates in five hydrogen bonds with the binding site of receptor (Fig. 10c). Similar to compound **5f**, the triazolyl group has a significant role in stabilizing **7b** in binding site since all nitrogens of triazolyl group establish three strong hydrogen bonds with OH of Tyr511. The hydroxyl of CHOH moiety of **7b** provides a strong hydrogen bond with OH of Thr550. This residue also provides another strong hydrogen bond with the eugenolyl group. The hydrophobic interactions between **7b** and binding site of TRPV1 were significantly achieved using Tyr511, Ser512, Leu515, Met547, Ala546, Leu553, Ile569, Val583, Phe587, Phe591, and Leu669 residues.

Ligand **11a** participates in establishing six strong hydrogen bonds with binding site of receptor (Fig. 10d). As observed for **5f** and **7b**, the nitrogen atoms of triazolyl

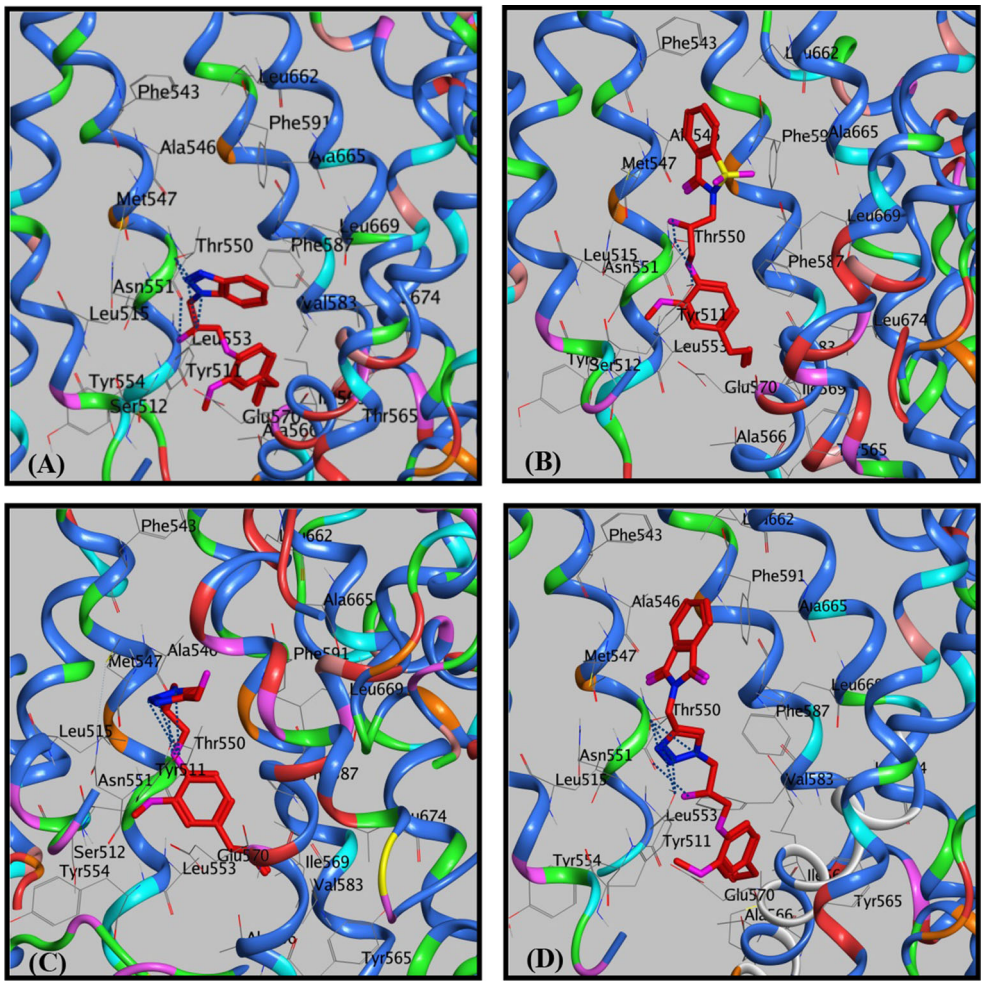

Fig. 10 Docked conformation and hydrogen bonds (dark blue) of **5f** (**a**), **5g** (**b**), **7b** (**c**), and **11a** (**d**) in binding site of TRPV1. (Color figure online)

group of **11a** participate in hydrogen bonds formation with residues at binding site. In this context, five strong hydrogen bonds between triazolyl group with Tyr511 and Thr550 were detected. It seems that the presence of triazolyl group can largely influence the proper binding of synthesized ligands with TRPV1 which results in good to excellent antinociceptive activity of these ligands. Apparently, this hypothesis was confirmed by obtained results from both experimental and docking studies. In addition, the hydroxyl group of **11a** forms a strong hydrogen bond with the carbonyl group of Thr550. Two hydrophobic pockets participate in hydrophobic interactions with **11a**. The first pocket is formed by Tyr511, Ser512, Leu515, Leu553, Tyr565, Ala566, Ile569, Val583, Phe587, and Leu669 which interacts with eugenolyl group. The second pocket which anchors in phthalimidyl group is formed by Phe543, Ala546, Met547, Phe591, Leu662, and Ala665.

Using MVD software, the calculated ΔG values for the interaction of capsaicin with TRPV1 and their hydrogen bond energy are − 134.53 and − 6.16 kcal/mol, respectively. The calculated ΔG values for the interaction of ligands **5f**, **5g**, **7b**, and **11a** with receptor are − 141.04, − 141.46, − 131.85, and − 168.30 kcal/mol, respectively. These ΔG values are strong evidence for binding of eugenyloxy propanol azole ligands at binding site of TRPV1. The total hydrogen bond energies for **5f**, **5g**, **7b**, and **11a** are − 14.19, − 8.93, − 13.41, and − 14.89 kcal/mol, respectively. The comparison of the values of total hydrogen bond energies of **5f**, **7b**, and **11a** with that of capsaicin and **5g** confirms that the presence of triazolyl groups plays a substantial role in binding of these ligands with TRPV1.

In silico pharmacokinetic profile

In recent decades, the developed approaches on the basis of in silico predictions have found a powerful tool for theoretical assessments of physiochemical properties [62]. In this connection, diverse physiochemical parameters and molecular descriptors were developed to estimate toxicity risks, drug likeness and drug scores in drug candidate molecules. An established concept by Lipinski, namely Lipinski's rule of five (RO5), emerged as a simple route to predict the drug likelihood for candidate drugs [63, 64].

Due to RO5, a drug candidate should (1) have a molecular weight less than 500 Dalton; (2) have an octanol–water partition coefficient value not more than 5; (3) include the hydrogen bond donors (sum of NH and OH) less than 5; (4) avoid more than 10 hydrogen bond acceptors (sum of N and O); and (5) exhibit 10 or fewer rotatable bonds. A drug candidate molecule that does not comply with these rules likely shows inferior pharmacokinetic profile for oral administration.

To investigate the in silico pharmacokinetic profile for synthesized compounds, we have employed a well-validate OSIRIS DataWarrior V4.7.1 freeware [65]. This software encompasses the database for commercial none drug molecules or traded drugs. The risks of side effects, such as mutagenic, tumourigenic, irritant and reproductive effects, can be estimated utilizing this software. The predicted toxicity risks by OSIRIS DataWarrior for all synthesized compounds are depicted in Table 3.

Table 3 Toxicity risks predicted by OSIRIS DataWarrior for all synthesized compounds

Compd.	Mutagenic	Tumourigenic	Reproductive effective	Irritant
5a	None	High	None	High
5b	None	High	None	High
5c	High	High	None	High
5d	High	High	None	High
5e	None	High	None	High
5f	High	High	None	High
5g	None	High	None	High
7a	None	High	None	High
7b	None	High	None	High
11a	None	High	None	High
11b	None	High	None	High
11c	None	High	None	High
Eugenol	High	High	None	High

As indicated in Table 3, in addition to eugenol as a reference drug, all synthesized compounds were predicted to involve the high risk of tumourigenic and irritant properties, whereas none of the studied compounds demonstrated the reproductive effective. Except that of compounds **5c**, **5d**, **5f** and eugenol that show the mutagenic risks, other studied compounds were anticipated to be harmless from mutagenic point of view (Table 3).

Aside from toxicity risks prediction by OSIRIS DataWarrior, this software is capable to determine some important physiochemical parameters or descriptors. In this connection, we calculated Lipinski's parameters to indicate whether compounds complied Lipinski's RO5 or not. As shown in Table 4, all computed molecular weights for synthesized compounds were ranged in 306–466 Dalton (< 500 g/mol). Additionally, except that of **11c**, the number of hydrogen bond acceptors (nHba) for all compounds were 5–10 which follows the RO5. The number of hydrogen bond donors (nHbd) = 1 and number of rotatable bonds (nrotb) = 8–10 were almost similar to commercial drugs which lie in range of RO5 (Table 4).

One of the most important parameters in Lipinski's RO5 is lipophilicity factor which traditionally is represented as an octanol–water partition coefficient (cLog P). This parameter is a descriptor for the affinity of unionized molecules or drugs for a lipophilic environment. Drugs with intense of lipophilicity values are unable to pass the blood–brain bar-

Table 4 Physicochemical properties predicted by OSIRIS DataWarrior software

Compd.	mw	nHba	nHbd	nrotb	cLog P	cLog S	TPSA	Drug likeness	Drug score
5a	288.346	5	1	8	1.6183	− 1.65	56.51	2.4166	0.3216
5b	338.406	5	1	8	3.0577	− 3.046	56.51	1.1508	0.2609
5c	364.444	5	1	9	3.2613	− 3.795	56.51	1.1548	0.1428
5d	347.370	8	1	9	1.1111	− 2.263	102.33	− 3.604	0.0990
5e	352.433	5	1	8	3.2911	− 2.674	56.51	1.1687	0.2596
5f	339.394	6	1	8	2.4726	− 3.324	69.4	− 3.7662	0.0917
5g	403.454	7	1	8	2.5996	− 2.972	101.52	4.1726	0.2840
7a	365.432	6	1	9	2.7834	− 3.706	69.4	− 3.1898	0.1460
7b	319.360	7	2	9	0.4899	− 1.836	89.63	− 3.1423	0.1733
11a	448.478	9	1	10	1.8393	− 3.284	106.78	− 1.6583	0.1560
11b	484.532	10	1	10	1.6293	− 2.78	132.23	0.4982	0.2111
11c	481.511	12	1	10	0.6067	− 2.27	127.84	− 1.5139	0.1592
Eugenol	164.203	2	1	3	2.2723	− 2.05	29.46	− 4.6405	0.1022

rier. Most known drugs are reported to have cLog P values < 5. The cLog P values for all synthesized compounds were calculated around 0.48–3.29 which are below the defined limit by RO5 (< 5). Among the title compounds, **5e** and **7b** was found to exhibit the maximal lipophilic and hydrophobic properties, respectively (Table 4). The aqueous solubility of a molecule or drug candidate (cLog S) is a main parameter that significantly affects absorption and distribution characteristics. Most established or traded drugs have a cLog *S* value > − 4. As can be seen in Table 4, all compounds have values more than indicated threshold value (> − 4). Topological or total polar surface area (TPSA) is a useful parameter for prediction of drug transport properties. TPSA is defined as a sum of surfaces of polar atoms (usually oxygen, nitrogen, and attached hydrogen) in a molecule. This parameter has been shown to correlate very well with the human intestinal absorption and blood–brain barrier penetration. In most common drugs, TPSA values were known to be less than 140 $Å^2$.

As shown in Table 4, all compounds involve TPSA values less than 140 $Å^2$. Fragment-based drug likeness is a parameter that is obtained from a fragment list which is prepared by the fragmentation of 3300 traded drugs as well as 15,000 commercially available chemicals to access a comprehensive list of all available fragments. Molecules that predominantly contain fragments that are often found in commercial drugs have a positive drug likeness. Among synthesized compounds, **5a–c**, **5e**, **5g** and **11b** exhibit positive drug likeness while the other compounds were found to involve negative values. Interestingly, the most negative values is obtained for eugenol as a reference drug. Among potent antinociceptive agents such as **5f**, **7b,** and **11a** and also all other tested derivatives, the maximum drug likeness was found for **5g**. The result of drug likeness as well as the above explained descriptors can be integrated to a parameter the so-called drug score. Drug score is a parameter that indicates whether a compound could be considered as a drug candidate or not. The higher drug score value means that compound has a more chance to be a drug candidate. Through the title compounds, nonetheless of their marginal biological activity, **5a** and **5d** were indicated to have maximum and minimum drug score values, respectively. Through antinociceptive compounds **5g**, **5f**, **7b,** and **11a,** compound **5g** showed the maximum drug score even more than eugenol. Regarding to appropriate drug likeness and drug score values of **5g** and also its remarkable antinociceptive activity, **5g** can be considered as a future drug candidate.

Conclusions

In summary, we explained the design and synthesis of novel eugenyloxy propanol azole derivatives. These compounds were in vivo examined for the acute antinociception on male Spargue Dawley rats using tail-flick test. The test results have revealed that compounds **5f**, **5g, 7b,** and **11a** displayed potent antinociceptive properties compare to eugenol as a reference drug. In this connection, at the time of maximal antinociceptive effect, i.e. 15 min. for **5f**, **5g**, **7b** and 30 min. for **11a**, the ratio of antinociceptive activity of **5f**, **5g**, **7b,** and **11a** to that of eugenol were found to be 2.3, 1.7, 1.9, and 1.7, respectively. Also, all compounds were ex vivo tested for β-adrenoceptor antagonist and/or agonist properties on isolated left atrium of male rats. This study has indicated that eugenyloxy propanol azole analogues involved partial antagonist or agonist behaviour compare to isoprenaline and propranolol as a reference β-agonist and antagonist agents, respectively. In silico molecular docking study was conducted for some of the analogues at the binding site of transient receptor potential vanilloid subtype 1 (TRPV1). The results have proved that

similar to capsaicin, the titled compounds show the strong affinity to bind at the site of TPRV1. Moreover, the presence of triazolyl moieties has played undeniable role in establishing durable binding of these ligands to TRPV1 and thus the significant factor for enhancing the analgesic activity of studied compounds compare to eugenol. The in silico pharmacokinetic profile, drug likeness and toxicity predictions were carried out for all compounds which determined that **5g** can be considered as potential analgesic drug candidate for further investigations.

Experimental

General

All materials as well as standard drugs involving isoprenaline, propranolol, and eugenol were purchased from either Sigma-Aldrich (UK), Fluka or Merck. All the chemical salts of PSS were used in analytical grade. The synthesized compounds were dissolved in pure dimethylsulphoxide (DMSO). Final concentration of DMSO in contact with preparation was up to 0.1% which had not any effect on responses in preliminary studies. Isoprenaline and propranolol were dissolved in distilled water. Solvents were purified using standard procedures and stored over 3 Å molecular sieves. Reactions were monitored by TLC using SILG/UV 254 silica-gel plates. Column chromatography was performed on silica gel 60 (0.063–0.200 mm, 70–230 mesh; ASTM). Melting points were measured using Electrothermal IA 9000 melting point apparatus in open capillary tubes and are uncorrected. IR spectra were obtained using a Shimadzu FT-IR-8300 spectrophotometer. ^{1}H- and ^{13}C-NMR spectra were recorded on a Brüker Avance DPX-250 spectrometer operating at 250/62.5 MHz, respectively. Chemical shifts are given in δ relative to tetramethylsilane (TMS) as an internal standard, and coupling constants J are given in Hz. Abbreviations used for ^{1}H NMR signals are *s* singlet, *d* doublet, *t* triplet, *q* quartet, *m* multiplet, *b* broad, *dd* doublet of doublet. GC/MS was performed on a Shimadzu GC/MS-QP 1000-EX apparatus (m/z; rel.%). Elemental analyses were performed on a Perkin–Elmer 240-B microanalyzer.

Animals

Male Spargue Dawley rats (200–220 g) were obtained from the Center of Comparative and Experimental Medicine, Shiraz University of Medical Sciences, Shiraz, Iran. All animals were kept in standard condition. The rats were randomly divided into 12 groups of synthesized compounds and a group of control. The experimental protocols were approved by the Ethics Committee of Shiraz University of Medical Sciences (Ethics committee approval number; ec-p-91-5317).

General procedure for the synthesis of Intermediates 3 and 4

To a round bottom flask (100 mL), equipped with a condenser, it was added a mixture of eugenol (0.01 mol), epichlorohydrin (0.02 mol), K_2CO_3 (0.01 mol), and tetrabutylammonium iodid (TBAI) (0.1 g) in CH_3CN (20 mL). The solution was heated to reflux for 10 h (TLC control). Then, the solvent was evaporated at reduced pressure, and the residue was dissolved in $CHCl_3$ (150 mL) and washed with H_2O (2 × 150 mL). The organic layer was dried (Na_2SO_4, 10 g) and evaporated. This adducts were used for the next step without further purification and separation.

General procedure for the synthesis of compounds (5a–g)

A solution of adducts **3** and **4** (0.01 mol) in CH_3CN (30 mL) was added into a flask containing mixture of appropriate *N*-heterocycle (0.01 mol), K_2CO_3 (0.01 mol), triethylamine (0.01 mol), and a catalytic amount of TBAI (0.1 g). The solution was heated to reflux for 10 h (Table 1). Then, the solvent was evaporated at reduced pressure, and the residue was dissolved in $CHCl_3$ (150 mL) and washed with H_2O (2 × 150 mL). The organic layer was dried (Na_2SO_4, 10 g) and concentrated to afford the crude product which was purified by column chromatography eluting with proper solvents.

General procedure for the synthesis of 1-(4-allyl-2-methoxy-phenoxy)-3-azido-propan-2-ol (6)

A mixture of adducts **3** and **4** (0.02 mol) with NaN_3 (0.04 mol) and acetone/H_2O 1:1 (30 mL) in a round bottom flask (100 mL) was stirred for 3 h (TLC control). Afterwards, acetone was evaporated at reduced pressure, and then, the crude product was dissolved in $CHCl_3$ (150 mL) and washed with H_2O (2 × 150 mL). The organic layer was dried (Na_2SO_4, 10 g) and concentrated to afford the crude product which was purified by column chromatography eluting with EtOAc–*n*-hexane (1:6).

Synthesis of propargyl tosylate (9)

In a round bottomed flask (100 mL) equipped with a mechanical stirrer was added propargyl alcohol (0.01 mol), tosyl chloride (0.02 mol), and diethyl ether (25 mL). The resulting reaction mixture was cooled in an ice bath, and NaOH (2 g, 0.05 mol) pellets were added to the solution in 6 portions at 0 °C under vigorous stirring. After the reaction completion (TLC control) and the evaporation of the organic solvent, the residue was dissolved in $CHCl_3$ (150 mL) and washed with H_2O (3 × 150 mL). The organic layer was dried (Na_2SO_4, 10 g) and concentrated to afford the crude product, which

was pure enough to use for the subsequent reaction without further purification.

General procedure for the synthesis of *N*-propargyl heterocycles (10)

In a round bottomed flask (100 mL), a mixture of the appropriate *N*-heterocycle (0.01 mol), propargyl tosylate (0.01 mol), and K_2CO_3 (0.01 mol) was dissolved in DMF (20 mL). Then, the mixture was stirred at room temperature for 10 h (TLC control). Afterwards, the solvent was evaporated at reduced pressure, and the residue was dissolved in $CHCl_3$ (150 mL) and washed with H_2O (3 × 150 mL). The organic layer was dried (Na_2SO_4, 10 g) and evaporated and then concentrated to afford the crude product which was purified by column chromatography eluting with proper solvents.

General procedure for the synthesis of compounds 7a, 7b, and 11a–c

To a round bottom flask (100 mL) was added a solution of **6** (0.01 mol), appropriate alkyne (0.01 mol), and a catalytic amount of CuI (0.1 g) in H_2O/THF 1:1 (30 mL). Then, the mixture was stirred at room temperature for 8 h (TLC control). Afterwards, the solvent was evaporated at reduced pressure, and the residue was dissolved in $CHCl_3$ (150 mL) and washed with H_2O (3 × 150 mL). The organic layer was dried (Na_2SO_4, 10 g) and evaporated and concentrated to afford the crude product which was purified by column chromatography eluting with proper solvents indicated below.

Data for compounds 5a–g, 7a, 7b and 11a–c

***1-(4-allyl-2*-methoxy-phenoxy*)-3-(1H-imidazol-1-yl) propan-2-ol* (5a)** This compound was obtained as a yellow oil using column chromatography on silica gel (EtOAc); Yield: 2.16 g, 75%; R_f = 0.17 (Methanol-EtOAc, 1:4); IR (film) ν_{max} = 3345, 3050, 2938, 1640, 1458, 1285, 1130 cm^{-1}; ^1H NMR ($CDCl_3$, 250 MHz): δ_{ppm} 3.23 (d, J = 6.7 Hz, 2H, $ArCH_2$), 3.73–3.79 (complex, 5H, OCH_3, NCH_2), 3.87–3.91 (m, 1H, CHOH), 4.03–4.20 (complex, 3H, OCH_2, OH), 4.96–5.03 (m, 2H, $=CH_2$), 5.78–5.91 (m, 1H, =CH), 6.74–6.95 (complex, 5H, aryl, C(4)-H and C(5)-H of imidazole), 7.45 (s, 1H, C(2)-H of imidazole); ^{13}C NMR ($CDCl_3$, 62.5 MHz): δ_{ppm} 38.74, 51.47, 55.16, 69.50, 72.13, 112.53, 113.82, 116.42, 120.87, 122.42, 128.95, 132.83, 137.04, 138.05, 147.91, 150.03; MS (EI): m/z (%) = 288 (19.5) [M^+]; Anal. Calcd for $C_{16}H_{20}N_2O_3$: C, 66.65; H, 6.99; N, 9.72. Found: C, 66.79; H, 7.17; N, 9.87.

***1-(4-allyl-2 methoxyphenoxy)-3-(1H-benzo[d] imidazole-1-yl) propan-2-ol* (5b)** This compound was obtained as a creamy solid using column chromatography on silica gel (EtOAc–*n*-hexane, 4:1); Yield: 2.77 g, 82%; mp 127–129 ^0C; R_f = 0.62 (Methanol-EtOAc, 1:4); IR (KBr) ν_{max} = 3300, 3028, 2954, 1662, 1450, 1282, 1148 cm^{-1}; ^1H NMR ($CDCl_3$, 250 MHz): δ_{ppm} 3.24 (d, J = 6.6 Hz, 2H, $ArCH_2$), 3.76 (s, 3H, OCH_3), 3.84–4.01 (m, 2H, NCH_2), 4.09–4.17 (m, 1H, CHOH), 4.25–4.33 (m, 1H, OCH_AH_B), 4.36 (dd, J = 3.2, 13.9 Hz, 1H, OCH_AH_B), 4.96–5.03 (m, 2H, $=CH_2$), 5.72–5.92 (complex, 2H, OH, =CH), 6.59–6.65 (m, 2H, aryl), 6.72 (d, J = 8.0 Hz, 1H, aryl), 7.00–7.08 (m, 2H, aryl), 7.30–7.40 (m, 2H, aryl), 7.77 (s, 1H, C(2)-H of benzimidazole); ^{13}C NMR ($CDCl_3$, 62.5 MHz): δ_{ppm} 38.25, 55.70, 56.74, 68.18, 72.35, 110.11, 112.94, 114.00, 115.81, 120.21, 122.85, 123.35, 123.87, 133.23, 135.08, 137.17, 143.12, 144.67, 147.29, 150.41; MS (EI): m/z (%) = 338 (24.1) [M^+]; Anal. Calcd for $C_{20}H_{22}N_2O_3$: C, 70.99; H, 6.55; N, 8.28. Found: C, 71.12; H, 6.70; N, 8.45.

***1-(4-allyl-2*-methoxy-phenoxy*)-3-(2-phenyl-1H-imidazol-1-yl) propan-2-ol* (5c)** This compound was obtained as a yellow oil using column chromatography on silica gel (EtOAc–*n*-hexane, 2:1); Yield: 2.77 g, 76%; R_f = 0.52 (Methanol-EtOAc, 1:2); IR (film) ν_{max} = 3250, 3065, 2983, 1668, 1471, 1268, 1143 cm^{-1}; ^1H NMR ($CDCl_3$, 250 MHz): δ_{ppm} 3.21 (d, J = 6.7 Hz, 2H, $ArCH_2$), 3.66–3.74 (complex, 5H, OCH_3, NCH_2), 3.95–4.20 (complex, 3H, OCH_2, CHOH), 4.95–5.02 (m, 2H, $=CH_2$), 5.15 (br s, 1H, OH), 5.77–5.90 (m, 1H, =CH), 6.56–6.59 (m, 3H, aryl), 6.87 (d, J = 1.1 Hz, 1H, C(5)-H of imidazole), 7.03 (d, J = 1.1 Hz, 1H, C(4)-H of imidazole), 7.22–7.24 (m, 3H, aryl), 7.42–7.46 (m, 2H, aryl);); ^{13}C NMR ($CDCl_3$, 62.5 MHz): δ_{ppm} 37.45, 50.34, 57.40, 68.97, 72.85, 113.32, 114.66, 116.46, 122.25, 125.11, 127.21, 128.29, 130.12, 130.65, 131.94, 133.25, 137.15, 148.47, 150.31, 154.53; MS (EI): m/z (%) = 364 (22.7) [M^+]; Anal. Calcd for $C_{22}H_{24}N_2O_3$: C, 72.50; H, 6.64; N, 7.69. Found: C, 72.36; H, 6.80; N, 7.81.

***1-(4-allyl-2*-methoxy-phenoxy*)-3-(2-methyl-4-nitro-1H-imidazol-1-yl) propan-2-ol* (5d)** This compound was obtained as a yellow solid using column chromatography on silica gel (EtOAc–*n*-hexane, 3:1); Yield: 2.70 g, 78%; mp 106–108 ^0C; R_f = 0.64 (Methanol-EtOAc, 1:10); IR (KBr) ν_{max} = 3200, 3074, 2986, 1667, 1548, 1463, 1350, 1285, 1142 cm^{-1}; ^1H NMR ($CDCl_3$, 250 MHz): δ_{ppm} 2.40 (s, 3H, CH_3), 3.32 (d, J = 6.6 Hz, 2H, $ArCH_2$), 3.84 (s, 3H, OCH_3), 3.95–4.31 (complex, 6H, NCH_2, OCH_2, CHOH), 5.04–5.11 (m, 2H, $=CH_2$), 5.88–6.02 (m, 1H, =CH), 6.70 (d, J = 7.7 Hz, 2H, aryl), 6.82 (d, J = 7.8 Hz, 1H, aryl), 7.87 (s, 1H, C(5)-H of imidazole); ^{13}C NMR ($CDCl_3$, 62.5 MHz): δ_{ppm} 13.07, 37.96, 50.51, 57.33, 69.62, 72.66, 112.49, 113.84, 116.25, 120.65, 121.36, 133.27, 137.06, 142.48, 147.91, 148.24, 150.65; MS (EI): m/z (%) = 347 (20.3) [M^+]; Anal. Calcd for $C_{17}H_{21}N_3O_5$: C, 58.78; H, 6.09; N, 12.10. Found: C, 58.90; H, 6.26; N, 12.29.

1-(4-allyl-2-*methoxy-phenoxy*)-3-(2-methyl-1H-benzo[d]imidazol-1-yl) propan-2-ol **(5e)** This compound was obtained as a creamy solid using column chromatography on silica gel (EtOAc–*n*-hexane, 3:1); Yield: 2.82 g, 80%; mp 155–157 ^{0}C; R_f = 0.50 (Methanol-EtOAc, 1:4); IR (KBr) ν_{max} = 3260, 3075, 2937, 1664, 1468, 1291, 1135 cm^{-1}; ^{1}H NMR (DMSO-d$_6$, 250 MHz): δ_{ppm} 2.57 (s, 3H, CH_3), 3.31 (d, J = 5.5 Hz, 2H, $ArCH_2$), 3.81–3.96 (complex, 5H, OCH_3, NCH_2), 4.18–4.26 (m, 2H, OCH_2), 4.39–4.45 (m, 1H, CHOH), 5.07–5.13 (m, 2H, =CH_2), 5.53 (s, 1H, OH), 5.93–6.04 (m, 1H, =CH), 6.69 (d, J = 7.7 Hz, 1H, aryl), 6.85–6.94 (m, 2H, aryl), 7.15 (br s, 2H, aryl), 7.52 (br s, 2H, aryl); ^{13}C NMR (DMSO-d$_6$, 62.5 MHz): δ_{ppm} 15.07, 40.78, 53.10, 57.30, 68.03, 71.97, 111.04, 113.14, 114.18, 116.01, 120.47, 122.06, 123.35, 123.88, 133.08, 136.48, 142.75, 143.28, 148.26, 149.05, 150.65; MS (EI): m/z (%) = 352 (26.2) [M$^+$]; Anal. Calcd for $C_{21}H_{24}N_2O_3$: C, 71.57; H, 6.86; N, 7.95. Found: C, 71.41; H, 6.73; N, 7.80.

1-(4-allyl-2-*methoxy-phenoxy*)-3-(1H-benzo[d] [1–3] triazol-1-yl)propan-2-ol **(5f)** This compound was obtained as a yellow solid using column chromatography on silica gel (EtOAc–*n*-hexane, 2:1); Yield: 2.34 g, 69%; mp 40–42 ^{0}C; R_f = 0.60 (EtOAc–*n*-hexane, 2:5); IR (KBr) ν_{max} = 3201, 3039, 2881, 1662, 1432, 1280, 1129 cm^{-1}; ^{1}H NMR ($CDCl_3$, 250 MHz): δ_{ppm} 2.88 (br s, 1H, OH), 3.29 (d, J = 6.5 Hz, 2H, $ArCH_2$), 3.79 (s, 3H, OCH_3), 3.91–3.98 (m, 1H, NCH_AH_B), 4.02–4.08 (m, 1H, NCH_AH_B), 4.52–4.58 (m, 1H, CHOH), 4.81–4.89 (m, 2H, OCH_2), 5.02–5.10 (m, 2H, =CH_2), 5.84–5.98 (m, 1H, =CH), 6.64–6.79 (m, 3H, aryl), 7.27–7.40 (m, 2H, aryl), 7.65–7.68 (m, 1H, aryl), 7.88–7.91 (d, J = 8.3 Hz, 1H, aryl); ^{13}C NMR ($CDCl_3$, 62.5 MHz): δ_{ppm} 39.84, 55.92, 58.85, 64.05, 72.92, 111.19, 112.68, 114.06, 116.91, 120.60, 122.40, 126.30, 126.81, 133.36, 134.13, 137.54, 145.84, 148.42, 150.25; MS (EI): m/z (%) = 339 (21.8) [M$^+$]; Anal. Calcd for $C_{19}H_{21}N_3O_3$: C, 67.24; H, 6.24; N, 12.38. Found: C, 67.43; H, 6.40; N, 12.52.

2-(3-(4-allyl-2-*methoxy-phenoxy*)-2-hydroxypropyl)benzo[d]isothiazol-3(2H)-one 1,1-dioxide **(5g)** This compound was obtained as a creamy foam using column chromatography on silica gel (EtOAc–*n*-hexane, 2:1); Yield: 3.23 g, 80%; R_f = 0.68 (EtOAc–*n*-hexane, 2:1); IR (film) ν_{max} = 3251, 3050, 2969, 1693, 1658, 1447, 1293, 1175, 1132 cm^{-1}; ^{1}H NMR ($CDCl_3$, 250 MHz): δ_{ppm} 3.23 (d, J = 6.7 Hz, 2H, $ArCH_2$), 3.45 (s, 1H, OH), 3.75 (s, 3H, OCH_3), 3.93–4.04 (complex, 4H, NCH_2, OCH_2), 4.30–4.36 (m, 1H, CHOH), 4.95–5.03 (m, 2H, =CH_2), 5.81–5.92 (m, 1H, =CH), 6.61–6.63 (m, 2H, aryl), 6.79 (d, J = 8.6 Hz, 1H, aryl), 7.74–7.96 (m, 4H, aryl); ^{13}C NMR ($CDCl_3$, 62.5 MHz): δ_{ppm} 40.13, 47.24, 57.23, 66.41, 72.50, 113.47, 114.54, 116.10, 121.90, 123.19, 124.25, 127.25, 133.72, 135.05, 136.35, 136.87, 141.08, 148.18, 150.01, 171.58; MS (EI): m/z (%) = 403 (23.5) [M$^+$]; Anal. Calcd for $C_{20}H_{21}NO_6S$: C, 59.54; H, 5.25; N, 3.47. Found: C, 59.40; H, 5.14; N, 3.60.

1-(4-allyl-2-*methoxy-phenoxy*)-3-(4-phenyl-1H-1, 2, 3-triazol-1-yl) propan-2-ol **(7a)** This compound was obtained as a white solid using column chromatography on silica gel (EtOAc–*n*-hexane, 2:1); Yield: 2.85 g, 78%; mp 96–98 ^{0}C; R_f = 0.60 (EtOAc–*n*-hexane, 2:1); IR (KBr) ν_{max} = 3253, 3042, 2971, 1670, 1427, 1231, 1152 cm^{-1}; ^{1}H NMR ($CDCl_3$, 250 MHz): δ_{ppm} 3.20 (d, J = 6.6 Hz, 2H, $ArCH_2$), 3.69 (s, 3H, OCH_3), 3.84–3.97 (m, 2H, NCH_2), 4.37–4.45 (complex, 2H, CHOH), 4.55 (dd, J = 2.5, 13.0 Hz, 2H, OCH_2), 4.93–5.01 (m, 2H, =CH_2), 5.77–5.88 (m, 1H, =CH), 6.57 (d, J = 7.6 Hz, 2H, aryl), 6.70 (d, J = 8.0 Hz, 1H, aryl), 7.12–7.27 (m, 3H, aryl), 7.57–7.61 (m, 2H, aryl), 7.80 (s, 1H, C(5)-H of triazole); ^{13}C NMR ($CDCl_3$, 62.5 MHz): δ_{ppm} 39.87, 57.26, 58.56, 66.35, 72.86, 113.04, 114.85, 116.67, 122.92, 127.82, 128.35, 129.37, 130.93, 131.46, 132.73, 137.67, 148.07, 149.11, 150.66; MS (EI): m/z (%) = 365 (24.1) [M$^+$]; Anal. Calcd for $C_{21}H_{23}N_3O_3$: C, 69.02; H, 6.34; N, 11.50. Found: C, 69.19; H, 6.20; N, 11.68.

1-(4-allyl-2-*methoxy-phenoxy*)-3-(4-(hydroxymethyl)-1H-1, 2, 3-triazol-1-yl) propan-2-ol **(7b)** This compound was obtained as a white solid using column chromatography on silica gel (EtOAc–*n*-hexane, 2:1); Yield: 2.40 g, 75%; mp 80–82 ^{0}C; R_f = 0.48 (EtOAc–*n*-hexane, 2:1); IR (KBr) ν_{max} = 3328, 3073, 2945, 1662, 1460, 1246, 1143 cm^{-1}; ^{1}H NMR ($CDCl_3$, 250 MHz): δ_{ppm} 3.29 (d, J = 6.4 Hz, 2H, $ArCH_2$), 3.80 (s, 3H, OCH_3), 3.90–4.01 (m, 2H, NCH_2), 4.38–4.47 (m, 3H, OCH_2, CHOH), 4.60 (s, 1H, CH_2OH), 4.65 (s, 2H, CH_2OH), 4.93–5.10 (complex, 3H, =CH_2, CHOH), 5.84–5.97 (m, 1H, =CH), 6.66 (d, J = 7.4 Hz, 2H, aryl), 6.78–6.85 (m, 1H, aryl), 7.72 (s, 1H, C(5)-H of imidazole); ^{13}C NMR ($CDCl_3$, 62.5 MHz): δ_{ppm} 40.38, 54.65, 57.78, 59.10, 66.35, 72.85, 113.96, 115.20, 117.06, 122.76, 129.54, 133.19, 138.13, 143.32, 148.75, 151.13; MS (EI): m/z (%) = 319 (15.6) [M$^+$]; Anal. Calcd for $C_{16}H_{21}N_3O_4$: C, 60.17; H, 6.63; N, 13.16. Found: C, 60.01; H, 6.79; N, 13.35.

2-((1-(3-(4-allyl-2-*methoxy-phenoxy*)-2-hydroxypropyl)-1H-1,2,3-triazol-4-yl)methyl)isoindoline-1,3-dione **(11a)** This compound was obtained as a yellow solid using column chromatography on silica gel (EtOAc–*n*-hexane, 1:1); Yield: 3.59 g, 80%; mp 99–97 ^{0}C; R_f = 0.43 (EtOAc–*n*-hexane, 1:4); IR (KBr) ν_{max} = 3339, 3060, 2947, 1698, 1661, 1429, 1272, 1150 cm^{-1}; ^{1}H NMR ($CDCl_3$, 250 MHz): δ_{ppm} 3.21 (d, J = 6.6 Hz, 2H, $ArCH_2$), 3.72–3.94 (complex, 6H, OCH_3, NCH_2CH, OH), 4.27–4.43 (complex, 2H, OCH_AH_B, CHOH), 4.52 (dd, J = 3.4, 11.8 Hz, 1H, OCH_AH_B), 4.87 (s, 2H, =CCH_2N), 4.95–5.02 (m, 2H, =CH_2), 5.76–5.92 (m, 1H, =CH), 6.57 (d, J = 7.4 Hz, 2H, aryl), 6.71 (d, J = 8.1 Hz,

1H, aryl), 7.58–7.62 (m, 2H, aryl), 7.69–7.74 (complex, 3H, aryl, C(5)-H of triazole); ^{13}C NMR ($CDCl_3$, 62.5 MHz): δ_{ppm} 40.73, 45.70, 57.21, 58.02, 66.41, 72.93, 113.01, 114.60, 116.93, 122.43, 124.02, 124.30, 125.82, 131.34, 132.68, 133.97, 137.65, 148.15, 150.20, 169.84; MS (EI): m/z (%) = 448 (29.7) [M^+]; Anal. Calcd for $C_{24}H_{24}N_4O_5$: C, 64.28; H, 5.39; N, 12.49. Found: C, 64.40; H, 5.23; N, 12.58.

2-((1-(3-(4-allyl-2-*methoxy-phenoxy*)-2-hydroxypropyl)-1H-1,2,3-triazol-4-yl)methyl)benzo[d]isothiazol-3(2H)-one 1,1-dioxide **(11b)** This compound was obtained as a yellow foam using column chromatography on silica gel (EtOAc–*n*-hexane, 1:1); Yield: 4.02 g, 83%; R_f = 0.50 (EtOAc–*n*-hexane, 5:1); IR (film) ν_{max} = 3350, 3037, 2976, 1697, 1663, 1464, 1283, 1167 cm^{-1}; ^{1}H NMR ($CDCl_3$, 250 MHz): δ_{ppm} 3.22 (d, J = 6.6 Hz, 2H, $ArCH_2$), 3.73–4.05 (3, 3H, OCH_3), 3.78–3.91 (complex, 3H, NCH_2CH) 4.27–4.45 (complex, 2H, OH, OCH_AH_B), 4.53 (dd, J = 3.7, 10.2 Hz, 1H, OCH_AH_B), 4.96–5.03 (complex, 4H, $=CCH_2N$, $=CH_2$), 5.79–5.90 (m, 1H, =CH), 6.58 (d, J = 7.8 Hz, 2H, aryl), 6.72 (d, J = 7.9 Hz, 1H, aryl), 7.73–7.82 (complex, 5H, aryl, C(5)-H of triazole); ^{13}C NMR ($CDCl_3$, 62.5 MHz): δ_{ppm} 39.76, 43.59, 56.76, 58.07, 65.91, 72.48, 112.70, 113.75, 116.38, 122.13, 122.68, 123.44, 124.46, 127.90, 131.02, 133.12, 135.20, 137.56, 137.81, 141.47, 148.27, 150.10, 171.28; MS (EI): m/z (%) = 484 (26.4) [M^+]; Anal. Calcd for $C_{23}H_{24}N_4O_6S$: C, 57.01; H, 4.99; N, 11.56. Found: C, 56.85; H, 4.87; N, 11.43.

7-((1-(3-(4-allyl-2-*methoxy-phenoxy*)-2-hydroxypropyl)-1H-1,2,3-triazol-4-yl)methyl)-1,3-dimethyl-1H-purine-2,6(3H,7H)-dione **(11c)** This compound was obtained as a white solid using column chromatography on silica gel (EtOAc–*n*-hexane, 2:1); Yield: 4.04 g, 84%; mp 100–102 ^{0}C; R_f = 0.50 (EtOAc–*n*-hexane, 5:1); IR (KBr) ν_{max} = 3342, 3053, 2962, 1712, 1696, 1653, 1461, 1260, 1149 cm^{-1}; ^{1}H NMR ($CDCl_3$, 250 MHz): δ_{ppm} 3.30–3.34 (complex, 5H, N(3)-CH_3, $ArCH_2$), 3.51 (s, 3H, N(1)-CH_3), 3.81 (s, 3H, OCH_3), 3.89–4.03 (complex, 3H, NCH_2CH), 4.45–4.53 (complex, 3H, OCH_2, OH), 5.04–5.10 (m, 2H, $=CH_2$), 5.54 (s, 2H, $=CCH_2N$), 5.87–5.98 (m, 1H, =CH), 6.66 (d, J = 7.8 Hz, 2H, aryl), 6.79 (d, J = 7.8 Hz, 1H, aryl), 7.80 (s, 1H, C(5)-H of triazole), 8.01 (s, 1H, C(8)-H of theophylline); ^{13}C NMR ($CDCl_3$, 62.5 MHz): δ_{ppm} 28.76, 29.81, 38.21, 45.31, 56.32, 58.14, 64.47, 70.77, 108.29, 112.47, 114.06, 116.17, 122.21, 123.25, 131.39, 133.24, 137.46, 147.14, 147.91, 149.25, 150.28, 152.37, 156.59; MS (EI): m/z (%) = 481 (27.2) [M^+]; Anal. Calcd for $C_{23}H_{27}N_7O_5$: C, 57.37; H, 5.65; N, 20.36. Found: C, 57.50; H, 5.81; N, 20.21.

Acknowledgements The authors wish to thank Shiraz University of Technology research council for partial support of this work. The authors are thankful from the High Performance Computing research laboratory of Institute for Research in Fundamental Sciences (IPM).

Compliance with ethical standards

Conflicts of interest The authors declare that they have no conflict of interest.

References

1. Nahin RL (2015) Estimates of pain prevalence and severity in adults: United States, 2012. J Pain 16:769–780. https://doi.org/10.1016/j.jpain.2015.05.002
2. Pain. https://en.wikipedia.org/wiki/Pain. Accessed 6 Jan 2018
3. Kingston DGI (2011) Modern natural products drug discovery and its relevance to biodiversity conservation. J Nat Prod 74:496–511. https://doi.org/10.1021/np100550t
4. Bhuiyan MNI, Begum J, Chandra Nandi N, Akter F (2010) Constituents of the essential oil from leaves and buds of clove (*Syzigium caryophyllatum* (L.) alston). Afr J Plant Sci 4:451–454
5. Schmalz G, Arenholt-Bindslev D (2009) Biocompatibility of dental materials. Springer, Heidelberg
6. Yogalakshmi B, Viswanathan P, Anuradha CV (2010) Investigation of antioxidant, anti-inflammatory and DNA-protective properties of eugenol in thioacetamide-induced liver injury in rats. Toxicology 268:204–212. https://doi.org/10.1016/j.tox.2009.12.018
7. Rojo L, Vazquez B, Roman JS, Deb S (2008) Eugenol functionalized poly(acrylic acid) derivatives in the formation of glass-ionomer cements. Dent Mater 24:1709–1716. https://doi.org/10.1016/j.dental.2008.04.004
8. Schmidt E, Jirovetz L, Wlcek K, Buchbauer G, Gochev V, Girova T, Stoyanova A, Geissler M (2007) Antifungal activity of eugenol and various eugenol-containing essential oils against 38 clinical isolates of Candida albicans. J Essent Oil Bear Plants 10:421–429. https://doi.org/10.1080/0972060x.2007.10643575
9. Prakash P, Gupta N (2005) Therapeutic uses of *Ocimum sanctum* linn (tulsi) with a note on eugenol and its pharmacological actions: a short review. Indian J Physiol Pharmacol 49:125–131
10. Awasthi PK, Dixit SC, Dixit N, Sinha AK (2008) Eugenol derivatives as future potential drugs. J Pharm Res 1:215–220
11. Burt SA, Reinders RD (2003) Antibacterial activity of selected plant essential oils against Escherichia coli O157:H7. Lett Appl Microbiol 36:162–167. https://doi.org/10.1046/j.1472-765x.2003.01285.x
12. Kim SI, Yi JH, Tak JH, Ahn YJ (2004) Acaricidal activity of plant essential oils against *Dermanyssus gallinae* (Acari: Dermanyssidae). Vet Parasitol 120:297–304. https://doi.org/10.1016/j.vetpar.2003.12.016
13. Li Y, Xu C, Zhang Q, Liu JY, Tan RX (2005) In vitro anti-helicobacter pylori action of 30 chinese herbal medicines used to treat ulcer diseases. J Ethnopharmacol 98:329–333. https://doi.org/10.1016/j.jep.2005.01.020
14. Pisano M, Pagnan G, Loi M, Mura ME, Tilocca MG, Palmieri G, Fabbri D, Dettori MA, Delogu G, Ponzoni M, Rozzo C (2007) Antiproliferative and pro-apoptotic activity of eugenol-related biphenyls on malignant melanoma cells. Mol Cancer 6(8):1–12. https://doi.org/10.1186/1476-4598-6-8
15. Zhao X, Chen D, Gao P, Ding P, Li K (2005) Synthesis of ibuprofen eugenol ester and its microemulsion formulation for parenteral delivery. Chem Pharm Bull 53:1246–1250. https://doi.org/10.1248/cpb.53.1246
16. Kaufman TS (2015) The multiple faces of eugenol. A versatile starting material and building block for organic and bio-organic synthesis and a convenient precursor toward bio-based fine chemicals. J Braz Chem Soc 26:1055–1085. https://doi.org/10.5935/0103-5053.20150086

17. Bendre RS, Rajput JD, Bagul SD, Karandikar PS (2016) Outlooks on medicinal properties of eugenol and its synthetic derivatives. Nat Prod Chem Res 4(3):100212–1000217. https://doi.org/10.4172/2329-6836.1000212
18. Fonseca-Berzal C, Ruiz FAR, Escario JA, Kouznetsov VV, Gómez-Barrio A (2014) In vitro phenotypic screening of 7-chloro-4-amino(oxy)quinoline derivatives as putative anti- Trypanosoma cruzi agents. Bioorg Med Chem Lett 24:1209–1213. https://doi.org/10.1016/j.bmcl.2013.12.071
19. Arango V, Domínguez JJ, Cardona W, Robledo SM, Muñoz SL, Figadere B, Sáez J (2012) Synthesis and leishmanicidal activity of quinoline–triclosan and quinoline–eugenol hybrids. Med Chem Res 21:3445–3454. https://doi.org/10.1007/s00044-011-9886-8
20. Chen H, Li G, Zhan P, Guo X, Ding Q, Wang S, Liu X (2013) Design, synthesis and biological evaluation of novel ligustrazinylated derivatives as potent cardiovascular agents. Med Chem Commun 4:827–832. https://doi.org/10.1039/c3md20352b
21. Hernández D, Bernal P, Cruz A, Garciafigueroa Y, Garduño L, Salazar M, Díaz F, Chamorro G, Tamariz J (2004) Potent hypolipidemic activity of mimetic amides of fibrates based on the 2-methoxy-4-(2-propenyl)phenoxyacetic scaffold. Drug Dev Res 61:19–36. https://doi.org/10.1002/ddr.10333
22. Huang YC, Wu BN, Yeh JL, Chen SJ, Liang JC, Lo YC, Chen IJ (2001) A new aspect of view in synthesizing new type beta-adrenoceptor blockers with ancillary antioxidant activities. Bioorg Med Chem 9:1739–1746. https://doi.org/10.1016/S0968-0896(01)00067-0
23. Bhat KI, Hussain MMM (2009) Synthesis, characterization and antimicrobial studies of some substituted pyrazolines from aryloxy acetyl hydrazine. Asian J Chem 21:3371–3375
24. Dallmeier K, Carlini EA (1981) Anesthetic, hypothermic, myorelaxant and anticonvulsant effects of synthetic eugenol derivatives and natural analogues. Pharmacology 22:113–127. https://doi.org/10.1159/000137479
25. Seixas Xavier FJ, da Franca Rodrigues KA, de Oliveira RG, Lima Junior CG, da Câmara RJ, Lima Keesen TS, de Oliveira MR, Lins Silva FP, de Almeida Vasconcellos MLA (2016) Synthesis and in vitro anti Leishmania amazonensis biological screening of Morita-Baylis-Hillman adducts prepared from eugenol, thymol and carvacrol. Molecules 21:1483. https://doi.org/10.3390/molecules21111483
26. Budavari S, O'Neil MJ, Smith A, Heckelman PE (2001) The merck index: an encyclopedia of chemicals, drugs, and biologicals, 13th edn. Merck & Co., Inc, Whitehouse Station
27. d'Avila Farias M, Oliveira PS, Dutra FSP, Fernandes TJ, de Pereira CMP, de Oliveira SQ, Stefanello FM, Lencina CL, Barschak AG (2013) Eugenol derivatives as potential anti-oxidants: is phenolic hydroxyl necessary to obtain an effect? J Pharm Pharmacol 66:733–746. https://doi.org/10.1111/jphp.12197
28. Abdul Rahim NHC, Asari A, Ismail N, Osman H (2017) Synthesis and antibacterial study of eugenol derivatives. Asian J Chem 29:22–26. https://doi.org/10.14233/ajchem.2017.20100
29. Chen SJ, Wang MH, Chen IJ (1996) Antiplatelet and calcium inhibitory properties of eugenol and sodium eugenol acetate. Gen Pharmacol 27:629–633. https://doi.org/10.1016/0306-3623(95)02089-6
30. Zhang P, Zhang E, Xiao M, Chen C, Xu W (2013) Enhanced chemical and biological activities of a newly biosynthesized eugenol glycoconjugate, eugenol α-d-glucopyranoside. Appl Microbiol Biotechnol 97:1043–1050. https://doi.org/10.1007/s00253-012-4351-2
31. Chen SJ, Huang YC, Wu BN, Chen IJ (1997) Eugenolol: AN eugenol-derived β-adrenoceptor blocker with partial β2-agonist and calcium mobilization inhibition associated vasorelaxant activities. Drug Dev Res 40:239–250. https://doi.org/10.1002/(sici)1098-2299(199703)40:3%3c239:aid-ddr4%3e3.0.co;2-l
32. A global brief on hypertension. http://apps.who.int/iris/bitstream/10665/79059/1/WHO_DCO_WHD_2013.2_eng.pdf. Accessed 6 Jan 2017
33. Staessen JA, Gasowski J, Wang JG, Thijs L, Hond ED, Boissel JP, Coope J, Ekbom T, Gueyffier F, Liu L, Kerlikowske K, Pocock S, Fagard RH (2000) Risks of untreated and treated isolated systolic hypertension in the elderly: meta-analysis of outcome trials. Lancet 355:865–872. https://doi.org/10.1016/s0140-6736(99)07330-4
34. Wilson CO, Gisvold O, Block JH (2004) Wilson and Gisvold's textbook of organic medicinal and pharmaceutical chemistry, 11th edn. Lippincott Williams & Wilkins, Philadelphia
35. Brunton LL, Lazo JS, Parker KL (2006) Goodman and Gilman's the pharmacological basis of therapeutics, 11th edn. McGraw-Hill, New York
36. Patrick GL (2001) An introduction to medicinal chemistry, 2nd edn. Oxford University Press, New York
37. Gorre F, Vandekerckhove H (2010) Beta-blockers: focus on mechanism of action. Which beta-blocker, when and why? Acta Cardiol 65:565–570. https://doi.org/10.1080/ac.65.5.2056244
38. Kleeman A, Engel J, Kutscher B, Reichert D (1999) Pharmaceutical substances, 3rd edn. Thieme, Stuttgart
39. El Hadri A, Nicolle E, Leclerc G, Pietri-Rouxel F, Strosberg AD, Archimbault P (2003) New series of N-substituted phenyl ketone oxime ethers: synthesis and bovine β3-adrenergic agonistic activities. Pharmazie 58:13–17
40. Soltani Rad MN, Behrouz S, Dianat M (2008) Aqueous-mediated ring opening of epoxides with oximes: a rapid entry into β-hydroxy oxime O-ethers as potential β-adrenergic blocking agents. Synthesis 13:2055–2064. https://doi.org/10.1055/s-2008-1067122
41. Soltani Rad MN, Behrouz S, Karimitabar F, Khalafi-Nezhad A (2012) 'Click synthesis' of some novel O-substituted oximes containing 1,2,3-triazole-1,4-diyl residues as new analogs of β-adrenoceptor antagonists. Helv Chim Acta 95:491–501. https://doi.org/10.1002/hlca.201100324
42. Soltani Rad MN, Behrouz S, Doroodmand MM, Movahediyan A (2012) Copper-doped silica cuprous sulfate (CDSCS) as a highly efficient and new heterogeneous nano catalyst for [3+2] Huisgen cycloaddition. Tetrahedron 68:7812–7821. https://doi.org/10.1016/j.tet.2012.07.032
43. Soltani Rad MN, Behrouz S, Movahedian A, Doroodmand MM, Ghasemi Y, Rasoul-Amini S, Ahmadi Gandomani A-R, Rezaie R (2013) Doped nano-sized copper(I) oxide (Cu_2O) on melamine-formaldehyde resin: a highly efficient heterogeneous nano catalyst for 'Click' synthesis of some novel 1H-1,2,3-triazole derivatives having antibacterial activity. Helv Chim Acta 96:688–701. https://doi.org/10.1002/hlca.201200224
44. Soltani Rad MN, Behrouz S, Zarenezhad E, Moslemin MH, Zarenezhad A, Mardkhoshnood M, Behrouz M, Rostami S (2014) Synthesis of fluorene and/or benzophenone O-oxime ethers containing amino acid residues and study of their cardiovascular and antibacterial effects. Med Chem Res 23:3810–3822. https://doi.org/10.1007/s00044-014-0967-3
45. Zhang Q, Ren H, Baker GL (2014) An economical and safe procedure to synthesize 2-hydroxy-4-pentynoic acid: a precursor towards 'clickable' biodegradable polylactide. Beilstein J Org Chem 10:1365–1371. https://doi.org/10.3762/bjoc.10.139
46. Asl MK, Nazariborun A, Hosseini M (2013) Analgesic effect of the aqueous and ethanolic extracts of clove. Avicenna J Phytomed 3:186–192
47. Park CK, Kim K, Jung SJ, Kim MJ, Ahn DK, Hong SD, Kim JS, Oh SB (2009) Molecular mechanism for local anesthetic action of eugenol in the rat trigeminal system. Pain 144:84–94. https://doi.org/10.1016/j.pain.2009.03.016
48. Daniel AN, Sartoretto SM, Schmidt G, Caparroz-Assef SM, Bersani-Amado CA, Cuman RKN (2009) Anti-inflammatory and antinociceptive activities A of eugenol essential oil in experimental

animal tests. Rev Bras Farmacogn 19:212–217. https://doi.org/10.1590/s0102-695x2009000200006
49. Tadiwos Y, Nedi T, Engidawork E (2017) Analgesic and anti-inflammatory activities of 80% methanol root extract of *Jasminum abyssinicum* Hochst. ex. Dc. (Oleaceae) in mice. J Ethnopharmacol 202:281–289. https://doi.org/10.1016/j.jep.2017.02.036
50. Schunck RVA, Macedo IC, Laste G, de Souza A, Valle MTC, Salomon JLO, Nunes EA, Campos ACW, Gnoatto SCB, Bergold AM, Konrath EL, Dallegrave E, Arbo MD, Torres ILS, Leal MB (2017) Standardized *Passiflora incarnata* L. extract reverts the analgesia induced by alcohol withdrawal in rats. Phytother Res 31:1199–1208. https://doi.org/10.1002/ptr.5839
51. Huang YC, Wu BN, Lin YT, Chen SJ, Chiu CC, Cheng CJ, Chen IJ (1999) Eugenodilol: a third-generation beta-adrenoceptor blocker, derived from eugenol, with alpha-adrenoceptor blocking and beta2-adrenoceptor agonist-associated vasorelaxant activities. J Cardiovasc Pharmacol 34:10–20. https://doi.org/10.1097/00005344-199907000-00003
52. Jara-Oseguera A, Simon SA, Rosenbaum T (2008) TRPV1: on the road to pain relief. Curr Mol Pharmacol 1:255–269. https://doi.org/10.2174/1874-470210801030255
53. Caterina MJ, Schumacher MA, Tominaga M, Rosen TA, Levine JD, Julius D (1997) The capsaicin receptor: a heat-activated ion channel in the pain pathway. Nature 389:816–824. https://doi.org/10.1038/39807
54. Tominaga M, Caterina MJ, Malmberg AB, Rosen TA, Gilbert H, Skinner K, Raumann BE, Basbaum AI, Julius D (1998) The cloned capsaicin receptor integrates multiple pain-producing stimuli. Neuron 21:531–543. https://doi.org/10.1016/s0896-6273(00)80564-4
55. Julius D (2013) TRP channels and pain. Annu Rev Cell Dev Biol 29:355–384. https://doi.org/10.1146/annurev-cellbio-101011-155833
56. Szallasi A, Blumberg PM (1990) Specific binding of resiniferatoxin, an ultrapotent capsaicin analog, by dorsal root anglion membranes. Brain Res 524:106–111. https://doi.org/10.1016/0006-8993(90)90498-z
57. Basbaum AI, Bautista DM, Scherrer G, Julius D (2009) Cellular and molecular mechanisms of pain. Cell 139:267–284. https://doi.org/10.1016/j.cell.2009.09.028
58. Liao M, Cao E, Julius D, Cheng Y (2013) TRPV1 structures in distinct conformations reveal activation mechanisms. Nature 504:113–118. https://doi.org/10.1038/nature12823
59. Darré L, Domene C (2015) Binding of capsaicin to the TRPV1 ion channel. Mol Pharm 12:4454–4465. https://doi.org/10.1021/acs.molpharmaceut.5b00641
60. Thomsen R, Christensen MH (2006) MolDock: a new technique for high-accuracy molecular docking. J Med Chem 49:3315–3321. https://doi.org/10.1021/jm051197e
61. Frisch MJ, Trucks GW, Schlegel HB, Scuseria GE, Robb MA, Cheeseman JR et al (2009) Gaussian 09, Revision A.01 Gaussian, Inc., Wallingford CT
62. Bienstock RJ (2011) Library design, search methods, and applications of fragment-based drug design. American Chemical Society, Washington
63. Lipinski CA, Lombardo F, Dominy BW, Feeney PJ (2001) Experimental and computational approaches to estimate solubility and permeability in drug discovery and development settings. Adv Drug Deliv Rev 46:3–26. https://doi.org/10.1016/s0169-409x(00)00129-0
64. Lipinski CA (2004) Lead- and drug-like compounds: the rule-of-five revolution. Drug Discov Today 1:337–341. https://doi.org/10.1016/j.ddtec.2004.11.007
65. Download DataWarrior V4.7.2. http://www.openmolecules.org/datawarrior/download.html. Accessed 2 Jan 2018